



# HHS Public Access

Author manuscript

Cell Rep. Author manuscript; available in PMC 2022 May 11.

Published in final edited form as:

Cell Rep. 2021 May 11; 35(6): 109107. doi:10.1016/j.celrep.2021.109107.

## A vaccine inducing solely cytotoxic T lymphocytes fully prevents Zika virus infection and fetal damage

Frank Gambino Jr.<sup>1,4</sup>, Wanbo Tai<sup>2,4</sup>, Denis Voronin<sup>2</sup>, Yi Zhang<sup>3</sup>, Xiujuan Zhang<sup>2</sup>, Juan Shi<sup>2</sup>, Xinyi Wang<sup>2</sup>, Ning Wang<sup>2</sup>, Lanying Du<sup>2,5,\*</sup>, Liang Qiao<sup>1,5,6,\*</sup>

<sup>1</sup>Department of Microbiology and Immunology, Stritch School of Medicine, Loyola University Chicago, Maywood, IL 60153, USA

<sup>2</sup>Lindsley F. Kimball Research Institute, New York Blood Center, New York, NY 10065, USA

<sup>3</sup>Biotherapy Center, The First Affiliated Hospital of Zhengzhou University, Zhengzhou, Henan 450052, China

<sup>4</sup>These authors contributed equally

<sup>5</sup>Senior author

<sup>6</sup>Lead contact

### SUMMARY

As vaccine-induced non-neutralizing antibodies may cause antibody-dependent enhancement of Zika virus (ZIKV) infection, we test a vaccine that induces only specific cytotoxic T lymphocytes (CTLs) without specific antibodies. We construct a DNA vaccine expressing a ubiquitinated and rearranged ZIKV non-structural protein 3 (NS3). The protein is immediately degraded and processed in the proteasome for presentation via major histocompatibility complex (MHC) class I for CTL generation. We immunize *Ifnar1*<sup>-/-</sup> adult mice with the ubiquitin/NS3 vaccine, impregnate them, and challenge them with ZIKV. Our data show that the vaccine greatly reduces viral titers in reproductive organs and other tissues of adult mice. All mice immunized with the vaccine survived after ZIKV challenge. The vaccine remarkably reduces placenta damage and levels of pro-inflammatory cytokines, and it fully protects fetuses from damage. CD8<sup>+</sup> CTLs are essential in protection, as demonstrated via depletion experiments. Our study provides a strategy to develop safe and effective vaccines against viral infections.

### Graphical Abstract

This is an open access article under the CC BY-NC-ND license (<http://creativecommons.org/licenses/by-nc-nd/4.0/>).

\*Correspondence: ldu@nybc.org (L.D.), lqiao@luc.edu (L.Q.).

#### AUTHOR CONTRIBUTIONS

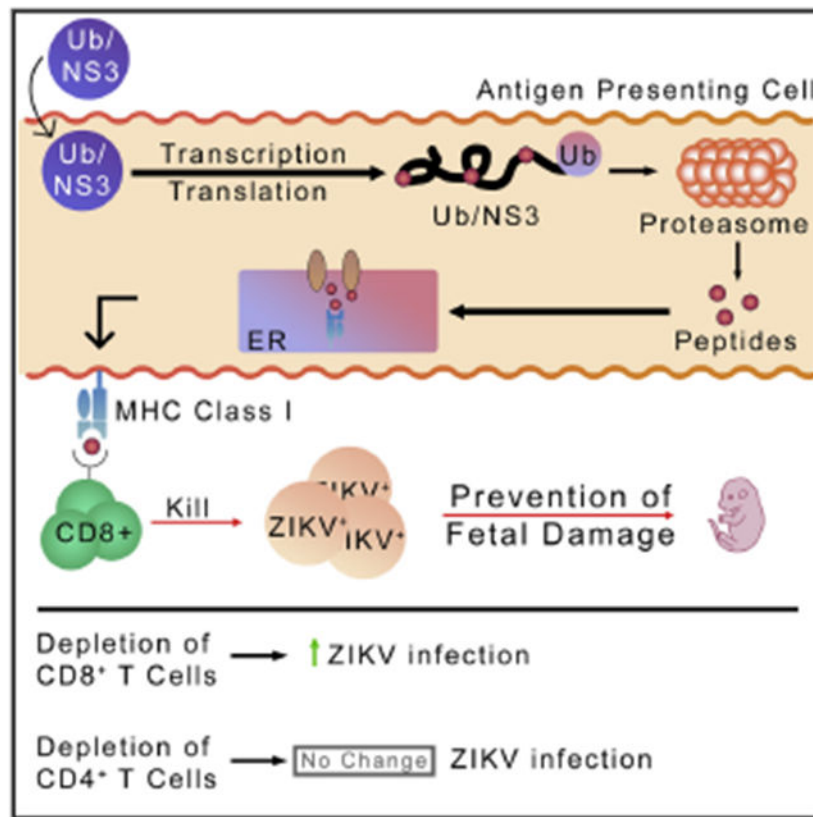
L.Q. and L.D. designed the project and wrote the manuscript with input from all authors. F.G. made the TCI vaccine, tested its expression and immunogenicity, and analyzed the data. W.T. immunized animals, performed viral challenge experiments, and analyzed the data. Y.Z. contributed to concept development. D.V., X.Z., J.S., X.W., and N.W. assisted with the experiments. L.Q. and L.D. evaluated the data and supervised the project.

#### SUPPLEMENTAL INFORMATION

Supplemental information can be found online at <https://doi.org/10.1016/j.celrep.2021.109107>.

#### DECLARATION OF INTERESTS

There are two patents pending: one US-based and one internationally. US Application No. 62/970,592; PCT International Application No. PCT/US2021/16654. Title: ZIKA VIRUS IMMUNOGENIC COMPOSITIONS.



### In brief

Non-neutralizing antibodies have been shown to enhance viral infection in flaviviruses. Gambino et al. sought a vaccine strategy that protects against ZIKV without inducing antibodies. They demonstrate that a ZIKV vaccine inducing solely NS3-specific CTLs provides full protection against ZIKV challenge and protects against fetal damage in pregnant mice.

## INTRODUCTION

Dengue virus (DENV) and Zika virus (ZIKV) belong to the family *Flaviviridae* (Lazear and Diamond, 2016). DENV has four serotypes that differ by 30%–35%, with their viral envelope (E) protein sequences differing from ZIKV E protein only by 41%–46% (Screaton et al., 2015). DENV infection usually does not cause severe symptoms but may lead to life-threatening complications such as dengue hemorrhagic fever (DHF) and dengue shock syndrome (DSS) (Khetarpal and Khanna, 2016). Primary infection by DENV leads to lifelong immunity to the infecting serotype, but not to the other serotypes (Murphy and Whitehead, 2011). Secondary infection by other serotypes is often responsible for DHF and DSS (Kalayanaraj, 2011). It is believed that the antibodies generated during primary DENV infection are unable to neutralize another serotype of the virus during secondary infection. These non-neutralizing antibodies instead bind to the virus and opsonize it into monocytes and macrophages via Fc-receptor-mediated endocytosis, leading to antibody-dependent enhancement (ADE) of infection. Similar to DENV infection, ZIKV infection

causes mild symptoms, if any, such as fever, myalgia, arthralgia, headache, conjunctivitis, and thrush in most infected people. However, severe symptoms such as microcephaly and other neurological abnormalities have been associated with ZIKV infection (Brasil et al., 2016; Cao-Lormeau et al., 2016; Driggers et al., 2016). Furthermore, it has been shown that human monoclonal antibodies generated from DENV-infected subjects cross-reacted with ZIKV (Priyamvada et al., 2016). Importantly, DENV-specific antibodies have been shown to enhance ZIKV pathogenesis and ZIKV-induced microcephaly-like syndrome in mice (Bardina et al., 2017; Dejnirattisai et al., 2016; Rathore et al., 2019). In addition, maternally acquired ZIKV-specific antibodies enhanced DENV infection and heightened disease states in mice (Fowler et al., 2018). It has also been demonstrated that preexisting high-antibody titers to DENV were associated with reduced risk of ZIKV infection and symptoms in humans (Rodriguez-Barraquer et al., 2019). Although it is unclear if the antibodies to DENV enhance ZIKV infection or provide protection against ZIKV infection, it may be prudent to design a vaccine that does not induce antibodies that may enhance either disease. Furthermore, vaccination with Dengvaxia, which expresses the precursor of membrane (prM) and E proteins from four serotypes of DENV, has led to more hospitalization of DENV-uninfected children than infected ones (a possible consequence of ADE) (Dans et al., 2018; Halstead, 2017; Martínez-Vega et al., 2017). This alarming result has prompted us to design a vaccine that does not induce potentially disease-enhancing antibodies.

A conventional vaccine is expected to induce neutralizing antibodies. However, it also induces non-neutralizing antibodies, which are responsible for ADE of DENV or ZIKV infection when neutralizing antibodies wane (Dejnirattisai et al., 2016; Langerak et al., 2019; Shim et al., 2019). It is very difficult to induce only neutralizing antibodies without non-neutralizing antibodies. We hypothesize that a ZIKV vaccine that elicits only ZIKV-specific cytotoxic T lymphocytes (CTLs), but not ZIKV-specific antibodies, will prevent ZIKV infection without the risk of ADE-mediated consequences. It is unknown whether CTLs are sufficient for full protection against a viral infection. It is traditionally believed that both neutralizing antibodies and CTLs are essential for prevention of a viral infection. Because humans mount significant T cell responses to ZIKV nonstructural protein 1 (NS1), NS3, and NS5 (Delgado et al., 2018; Herrera et al., 2018a, 2018b) and dominant CTL responses to NS3 and NS5 (Edupuganti et al., 2017; El Sahly et al., 2018; Waggoner et al., 2017), we designed a vaccine that targets ZIKV NS3. Furthermore, we used a ubiquitination and gene rearrangement strategy to enhance the degradation of NS3 in the proteasome with the goal of inducing only NS3-specific CTLs. We tested the efficacy of this vaccine in protection against ZIKV challenge in animal models.

## RESULTS

### TCI ZIKV vaccine design

Great efforts have been made to develop vaccines to prevent ZIKV infection. These vaccine candidates range from live-attenuated viruses to viral vectors, mRNA, and DNA (Abbink et al., 2016, 2017; Brault et al., 2017; Bullard et al., 2018; Dowd et al., 2016; Gaudinski et al., 2018; Griffin et al., 2017; Grubor-Bauk et al., 2019; Jagger et al., 2019; Larocca et al., 2016, 2019; Pardi et al., 2017; Richner et al., 2017a, 2017b; Van Rompay et al.,

2019; Shan et al., 2017; Tebas et al., 2017). In several of these studies, prM and E proteins have been targeted, albeit with considerably differing amino acid sequences across strains. A predictive epitope analysis found that all CD8<sup>+</sup> T cell epitopes on the NS3 amino acid sequence were conserved across 54 different ZIKV genomes (Dar et al., 2016; Mirza et al., 2016). Normally, the NS3 protein is covalently bonded to NS2B, an anchor protein that functions as a cofactor to promote the productive folding and activity of NS3 (Phoo et al., 2016). The N-terminal region of the NS3 protein encodes for a serine protease, while the latter region encodes for a helicase. This ZIKV NS2B-NS3pro complex is responsible for the cleavage of the ZIKV polyprotein precursor and the generation of the other proteins in the ZIKV viral genome (Hilgenfeld et al., 2018; Lei et al., 2016; Li et al., 2017; Phoo et al., 2018). As the NS3 protein is essential for the functionality of every other ZIKV viral protein, and its CD8<sup>+</sup> T cell epitopes are conserved across 54 different ZIKV genomes (Dar et al., 2016), this protein serves as an attractive target for vaccine therapy. Thus, we used NS3 as the target protein in our T-cell-inducing (TCI) ZIKV vaccine.

First, we split the NS3 gene (PRVABC59/2015 strain of ZIKV in *Homo sapiens*) into three parts and rearranged them (Figure 1A) in order to disrupt NS3's viral functions. Furthermore, this rearrangement may produce an unstable protein, which will be likely targeted to the proteasome for degradation. In constructing this sequence, the 30 nucleotide bases before and after any cleaved sites were placed back to preserve any CTL epitopes that may have been disrupted. The open reading frame (ORF) encoding for a mouse/human monomer of ubiquitin (Ub) was placed immediately upstream of the rearranged NS3 DNA sequence. A glycine at the 76th residue was modified to encode an alanine to enhance the stability of the Ub/NS3 complex (Figure 1A), which has been shown to promote protein degradation in the proteasome (Rodriguez et al., 1997). In order to ensure efficient transcription, a Kozak sequence was placed upstream of this combined Ub/NS3 sequence. The rearranged Ub/NS3 sequence was inserted into pVAX1, an FDA-approved vector for use in DNA vaccines in humans.

To determine the expression of the rearranged NS3, the plasmid DNA was used to transfect 293T cells. RNA was isolated, and RNA reverse transcription was conducted. Quantitative reverse transcription PCR (qRT-PCR) was conducted using primers specific to the Ub/NS3 sequence. NS3 gene transcription was confirmed (Figures S1A and S1B). We further determined expression of the NS3 protein. Naturally, there comes a problem with visualizing a protein that is innately ubiquitinated. It is widely known that many proteins are targeted for degradation by covalent ligation to ubiquitin (Schrader et al., 2009). Therefore, any protein that is innately ubiquitinated is targeted for immediate destruction. To address this issue, we used proteasome inhibitor MG132. Thus, 293T cells were transfected overnight with the plasmid DNA delivered in polyethylenimine (PEI) transfection reagent. The 293T cells were allowed to stably express the transfected protein for 36 h. After this period, cells were treated with 50  $\mu$ M MG132 overnight. A western blot was then conducted to determine the production of the rearranged Ub/NS3 protein (Figure 1B), and band intensity was quantified via ImageJ (Figure 1C). In transfected cells not treated with MG132, there is very low band intensity at 70 kDa, indicating that the Ub/NS3 protein is either not translated or it is targeted for immediate degradation. When cells are treated with MG132, however, band intensity increases tremendously. These data not only confirm the translation of the Ub/NS3

protein, but by inhibiting the proteasome, also demonstrate that the translated protein would have been targeted for immediate degradation otherwise (Figure 1C).

### **ZIKV TCI-DNA vaccine protected female pregnant BALB/c mice and their fetuses against ZIKV challenge**

To investigate the efficacy of our ZIKV TCI-DNA vaccine in protecting pregnant mothers and their fetuses against ZIKV infection, we first tested the immunogenicity of this vaccine in immunocompetent mice, as interferon (IFN)- $\alpha/\beta$  receptor (IFNAR)-knockout mice (the current mouse model for ZIKV challenge) may have a reduced ability to generate CTLs. Thus, we immunized immunocompetent female BALB/c mice (non-lethal to ZIKV infection) with TCI-DNA in the presence of Imiquimod adjuvant, ZIKV E ectodomain, EDI/II peptides in the presence of aluminum hydroxide (Alum) and monophosphoryl lipid A (MPL) adjuvants, or PBS. We used E ectodomain (Aviva Systems Biology) as a control immunogen because it is expected to induce E-protein-specific antibodies that may result in ADE. E ectodomain should be recognized by B cells and processed in antigen-presenting cells for presentation to CD4<sup>+</sup> and CD8<sup>+</sup> T cells. The peptide control immunogen (EDI/II peptides) is made of long peptides that contain major histocompatibility complex (MHC)-class-I-restricted epitopes including H-2 D<sup>b</sup>, K<sup>b</sup>-, and K<sup>d</sup>-restricted epitopes (no MHC-class-II-restricted epitopes), which are confirmed in animal studies. EDI/II peptides are expected to induce only CTLs but are less immunogenic than our TCI vaccine. Ten days after the second immunization, the female mice were mated with males. It took 2–3 weeks for the mice to be impregnated. After the female mice were impregnated (embryonic day [E]5–E7), they were injected with anti-IFNAR1 antibody (to make the mice susceptible to ZIKV by blocking IFNARs) (Gorman et al., 2018; Morrison and Diamond, 2017; Wang et al., 2019). One day later, mice were challenged with a high dose of ZIKV (R103451,  $2 \times 10^5$  plaque-forming unit [PFU]) and examined for morphological changes of uteri 6 days after. Mouse placenta and amniotic fluid were also evaluated for ZIKV titers via plaque-forming assay (Figure S2A).

The uteri (E11–E13) from TCI-DNA and E-ectodomain-immunized pregnant BALB/c mice exhibited normal morphology without obvious fetal death, indicating complete protection against uteri damage and fetal death; in contrast, EDI/II-peptide- or PBS-injected pregnant mice had either slightly or severely damaged uteri with reduced size, indicating fetal death and incomplete protection against ZIKV infection (Figure S3A). Investigation of viral titers in ZIKV-infected placenta and amniotic fluid revealed undetectable or significantly lower titer of ZIKV in placenta (Figure S3B) and amniotic fluid (Figure S3C) of mice receiving TCI-DNA vaccine than in those of mice receiving E ectodomain, EDI/II peptides, or PBS. In addition, there were significant but slightly lower viral titers in the placenta of mice immunized with E ectodomain than in those of mice injected with PBS (Figure S3B). Collectively, these results suggest that the TCI-DNA vaccine completely protected immunocompetent pregnant mice and their fetuses against high-dose challenge of ZIKV R103451, a human strain responsible for the recent ZIKV outbreaks (Tai et al., 2018). Because we challenged the pregnant mice with ZIKV >30 days after the last immunization, we concluded that the protection was due to the vaccine-induced immune memory.

## ZIKV TCI-DNA vaccine protected ZIKV-susceptible adult or pregnant *Ifnar1*<sup>-/-</sup> mice and their fetuses against two different strains of ZIKV challenge

Because there is no disease pathology in wild-type adult mice challenged with the ZIKV, we used a lethal mouse model to test our vaccine efficacy. Thus, we immunized *Ifnar1*<sup>-/-</sup> mice, an IFNAR-deficient mouse model lethal to ZIKV (Marzi et al., 2018; Tai et al., 2018, 2019a), with TCI-DNA, ZIKV E ectodomain, EDI/II peptides, or PBS as described above and performed the following three challenge experiments (Figure S2A).

First, we challenged IFNAR-deficient immunized adult (male and female) mice with ZIKV (strain R103451, 10<sup>3</sup> PFU) 10 days post-last dose and monitored their weight and survival changes for 14 days. We found that mice immunized with TCI-DNA had only slight weight loss during days 7–9 post-challenge, followed by constantly increased weight until 14 days (Figure 2A), and all mice from this group survived ZIKV challenge (Figure 2B). In contrast, the mice immunized with E ectodomain or EDI/II peptides showed reduced survival rates (to about 83% and 50%, respectively), and their weight either slightly or moderately decreased (Figures 2A and 2B). Mice injected with PBS had continuously decreased weight, and all mice died at 8 days post-challenge (Figures 2A and 2B). These data confirm complete protection of TCI-DNA vaccine against ZIKV-caused death and weight loss.

Second, we challenged immunized adult (male and female) *Ifnar1*<sup>-/-</sup> mice with ZIKV PAN2016 (10<sup>3</sup> PFU/mouse), another human strain causing recent ZIKV outbreaks (Gao et al., 2019; Tai et al., 2018), and measured ZIKV titers in sera and tissues via plaque-forming assay 6 days later. We noted undetectable viral titers in the lung, muscle, and testis of mice immunized with TCI-DNA, and viral titers in the sera and most tissues of these mice were also significantly lower than in those of mice immunized with E ectodomain, EDI/II peptides, or PBS (Figure 2C). In addition, ZIKV titers in sera, brain, lung, spleen, muscle, or testis of mice receiving E ectodomain or EDI/II peptides were also significantly lower than in those of mice injected with PBS (Figure 2C). These data indicate that the TCI-DNA vaccine significantly enhanced this protection, resulting in undetectable or significantly decreased viremia and viral titers in key organs, including reproductive organs such as testis.

Third, immunized female *Ifnar1*<sup>-/-</sup> mice were mated with male *Ifnar1*<sup>-/-</sup> mice for pregnancy (E5–E7) and were challenged with ZIKV (strain R103451; 10<sup>4</sup> PFU/mouse) as we did for BALB/c mice. Mice were then examined for morphological changes of uteri and fetuses, as well as viral titers in sera, amniotic fluid, fetal brain, and tissues at 6 days post-challenge. The uteri from TCI-DNA-immunized pregnant *Ifnar1*<sup>-/-</sup> mice had intact morphology and normal fetuses without demise, whereas the uteri from mice immunized with E ectodomain or EDI/II peptides exhibited slight or severe damage, with moderate and severe fetal resorption or fetal death in uteri, respectively (Figure 3A). Different from other groups, almost all fetuses survived from uteri of TCI-DNA-immunized pregnant mice after ZIKV challenge (Figure 3B). Importantly, viral titers in the placenta, amniotic fluid, and fetal brain (Figures 3C and 3D) of mice receiving the TCI-DNA vaccine were either undetectable or significantly lower than in those of mice receiving E ectodomain, EDI/II peptides, or PBS. Also, there were significantly lower titers of ZIKV in the placenta, amniotic fluid, and fetal brain of mice immunized with E ectodomain and EDI/II peptides than in those of mice injected with PBS (Figures 3C and 3D). Notably, ZIKV titers in the muscle, brain, heart,

liver, and spleen of mice immunized with TCI-DNA were undetectable or significantly lower than in those of mice immunized with E ectodomain, EDI/II peptides, or PBS, and viral titers in the sera and kidney of TCI-DNA-immunized mice were also significantly lower than in those of mice receiving EDI/II peptides or PBS (Figures 3C and 3D). Moreover, the results also denoted significantly lower viral titers in the sera and tissues (kidney, heart, liver, spleen, and muscle) of mice vaccinated with E ectodomain than in those of mice injected with PBS (Figures 3C and 3D).

Collectively, the above data confirm that the TCI-DNA vaccine completely protected adult or pregnant *Ifnar1<sup>-/-</sup>* mice and their fetuses against two different strains of ZIKV infection.

### **ZIKV TCI-DNA vaccine prevented ZIKV-caused apoptosis, vascular damage and inflammation, and ZIKV-associated ADE**

ZIKV infection may cause apoptosis and fetal blood vessel damage in placenta, leading to severe inflammation with increased cytokines and chemokines (He et al., 2018; Miner et al., 2016; Rabelo et al., 2018; Souza et al., 2016; Tripathi et al., 2017). It is reported that ZIKV E protein, including fusion loop (FL) region, may induce cross-reactive antibodies that enhance ZIKV or DENV infection, resulting in ADE (Barba-Spaeth et al., 2016; Barbosa et al., 2018; Fowler et al., 2018).

To evaluate whether the ZIKV TCI-DNA vaccine can prevent apoptosis and vasculature damage associated with ZIKV, we performed immunofluorescence staining using placental tissues of vaccine-immunized and ZIKV-challenged pregnant *Ifnar1<sup>-/-</sup>* mice (as described above) and stained for active caspase-3, an apoptotic marker (Yuan et al., 2017), and vimentin, a marker for fetal blood vessels and fetal capillary endothelium (Miner et al., 2016; Sapparapu et al., 2016). There were significantly lower numbers of caspase-3<sup>+</sup> and ZIKV<sup>+</sup> signals in the placenta of mice immunized with the TCI-DNA vaccine than in those of mice immunized with E ectodomain, EDI/II, or PBS (Figures 4A-4C), suggesting nearly no ZIKV-associated cell death in the TCI-DNA-immunized mouse placenta. In contrast, there was moderate to strong staining of caspase-3 and ZIKV in the placenta from other groups (E ectodomain, EDI/II, or PBS) (Figures 4A-4C), illustrating that E ectodomain or EDI/II may not fully prevent ZIKV-related cell death. Furthermore, there was strong staining for vimentin in the placenta of mice immunized with TCI-DNA (Figure S4A), with significantly higher numbers of vimentin<sup>+</sup> signals than those of mice receiving E ectodomain, EDI/II, or PBS (Figures S4B and S4C), suggesting intact vasculature in the TCI-DNA-vaccinated mouse placenta but partially or completely damaged vasculature in the placenta of other groups.

To examine whether ZIKV TCI-DNA vaccine can prevent ZIKV-caused inflammation, we measured inflammatory cytokines and chemokines in the placenta of immunized and ZIKV-infected pregnant *Ifnar1<sup>-/-</sup>* mice using Multi-Analyte ELISArray kits. Significantly lower levels of cytokines (interleukin [IL]-1 $\alpha$ , IL-1 $\beta$ , IL-6, IL-10, G-CSF, and GM-CSF) (Figure 5A) and chemokines (MCP-1, SDF-1, IP-10, MIG, Eotaxin, KC, and 6CKine) (Figure 5B) were identified in the TCI-DNA-immunized mouse placenta than in the placenta of mice immunized with EDI/II, E ectodomain or PBS. These results indicate that TCI-DNA is effective in preventing ZIKV-associated inflammation.

To investigate whether the ZIKV TCI-DNA vaccine may induce ZIKV-specific antibodies and, if so, whether these antibodies can cause ZIKV-associated ADE, we measured antibodies by ELISA and plaque-forming assay and tested for ADE *in vitro* using immunized sera of BALB/c and *Ifnar1*<sup>-/-</sup> mice. Clearly, no or a very low level of immunoglobulin G (IgG) antibodies was detected against ZIKV E ectodomain, NS3 peptides, and/or ZIKV lysates in the sera of both mice immunized with TCI-DNA (Figures 6A and 6B), and there were no neutralizing antibodies detected against ZIKV infection in these sera (Figure 6C). Moreover, similar to the sera collected from PBS-injected mice, TCI-DNA-immunized mouse sera did not present any ADE (Figure 6D). In contrast, ZIKV E ectodomain elicited high-level E- and ZIKV-specific IgG antibodies with neutralizing activity against ZIKV infection, exhibiting strong ADE of ZIKV infection (Figure 6). However, the ADE showed up only when the sera was diluted until the neutralizing activity was gone. These data demonstrate that TCI-DNA did not induce ZIKV E-specific antibodies but only elicited very weak NS3-specific antibody responses, eliminating the possibility of causing ZIKV-associated ADE.

Collectively, the above results confirm that the ZIKV TCI-DNA vaccine demonstrated the ability to prevent ZIKV-associated apoptosis, vascular damage, and inflammation without leading to ADE.

### **ZIKV TCI-DNA-vaccine-induced CD8<sup>+</sup> T cells play a key role in protecting adult or pregnant mice and their fetuses against ZIKV infection**

Since ZIKV TCI-DNA induced very low to no antibody responses, we then tested whether the T cell responses elicited by this vaccine were essential in protecting against ZIKV infection. As such, we performed the following two experiments (Figure S2B).

First, we immunized immunocompetent male and female BALB/c mice with TCI-DNA or PBS control and then depleted their CD4<sup>+</sup> and CD8<sup>+</sup> T cells, respectively (using anti-CD4 or anti-CD8a antibody), followed by ZIKV challenge. There were minimal numbers of CD4<sup>+</sup> or CD8<sup>+</sup> T cells in the peripheral blood cells and splenocytes of anti-CD4- or anti-CD8a-treated, TCI-DNA-, or PBS-immunized mice compared to those of mice treated with isotype antibody control (Figures S5A and S5B), confirming complete depletion of CD4<sup>+</sup> or CD8<sup>+</sup> T cells in these mice. Compared to PBS control, the mice immunized with TCI-DNA have significantly more CD8<sup>+</sup> T cells, as seen in the mice receiving anti-CD4 or isotype control antibody (no CD8<sup>+</sup> T cell depletion) (Figures S5A and S5B). In contrast, the mice immunized with TCI-DNA have similar numbers of CD4<sup>+</sup> T cells as control mice, as seen in the mice receiving anti-CD8a or isotype control antibody (no CD4<sup>+</sup> T cell depletion) (Figures S5A and S5B). In addition, high viral titers were detected in the sera and tissues (lung, eye, and muscle) of mice immunized with the TCI-DNA vaccine, and CD8<sup>+</sup> T cells depleted, which were significantly higher than those of TCI-DNA-immunized mice injected with anti-CD4 or isotype control antibody (no CD8<sup>+</sup> T cell depletion) (Figure S5C). In contrast, there were no significant differences in viral titers in the mice immunized with TCI-DNA who received either anti-CD4 (CD4<sup>+</sup> T cell depletion) or isotype control antibody (Figure S5C). These data suggest that CD8<sup>+</sup> T cells in TCI-DNA-immunized adult mice are essential in the prevention of ZIKV infection.

Second, we evaluated the role of CD8<sup>+</sup> T cells induced by TCI-DNA in protecting pregnant mice and their fetuses against ZIKV challenge. As such, we immunized female BALB/c mice with TCI-DNA or PBS control, mated them with male BALB/c mice for pregnancy, and then depleted their CD8<sup>+</sup> T cells before ZIKV challenge. Depletion of CD8<sup>+</sup> T cells was confirmed by flow cytometry analysis in the whole blood of mice 6 h before and 3 days after ZIKV challenge.

We compared the uteri status, fetal damage, and virus titers in the mice with or without CD8<sup>+</sup> T cell depletion. In the mice immunized with the TCI-DNA vaccine, we found significantly damaged uteri and severe fetal demise when their CD8<sup>+</sup> T cells were depleted, whereas intact uteri and fetuses without any damage were found when the mice were injected with isotype control antibody (no CD8<sup>+</sup> T cell depletion) (Figure 7A). The mice receiving PBS and injected with anti-CD8a or isotype control antibody exhibited different degrees of uteri damage and/or fetal death (Figure 7A). In addition, at least half of the fetuses died in the uteri of CD8<sup>+</sup> T-cell-depleted mice, whereas almost all fetuses survived in those of TCI-DNA-immunized mice receiving isotype control antibody (Figure 7B). Moreover, CD8<sup>+</sup> T cell depletion led to significantly increased ZIKV titers in the placenta, amniotic fluid, and fetal brain, as well as day 3 or day 6 post-infection (p.i.) in sera (Figure 7C) in the TCI-DNA-immunized pregnant mice and their fetuses. These data showed enhanced infection of TCI-DNA-vaccinated pregnant mice to ZIKV after their CD8<sup>+</sup> T cells were depleted.

We further evaluated ZIKV-specific CD8<sup>+</sup> T cell responses using flow cytometry analysis in the TCI-DNA-immunized and ZIKV-challenged pregnant mice without CD8<sup>+</sup> T cell depletion (i.e., mice receiving isotype antibody). To do this, splenocytes were isolated from these mice 6 days post-challenge and stimulated with ZIKV NS3 overlapping peptides. Remarkably, TCI-DNA elicited ZIKV-specific CD8<sup>+</sup> T cell responses (Figure 7D, left), being able to secrete high-level IL-2, IFN- $\gamma$ , and TNF- $\alpha$  cytokines; however, PBS control induced only a background level of these cytokines (Figure 7D, right).

Collectively, the above data demonstrate that ZIKV TCI-DNA-vaccine-induced CD8<sup>+</sup> T cells play an essential role in protecting adult, pregnant mice and their fetuses against ZIKV infection and/or ZIKV-associated fetal damage and death.

## DISCUSSION

Since a ZIKV vaccine targeting prM and E proteins may induce ADE, investigators have tested an innovative approach to use NS1 as a ZIKV vaccine target antigen for the prevention of ZIKV infection (Brault et al., 2017; Grubor-Bauk et al., 2019; Rodriguez et al., 1997). Immunization with ZIKV NS1 expressed by an MVA vector protected immunocompetent mice against a lethal intracerebral dose of ZIKV challenge (Brault et al., 2017). However, it is unclear whether the protection was dependent on T cells or antibodies. It has been shown that T cell immunity induced by a DNA vaccine expressing ZIKV NS1 played a crucial role in the early control of viral titers in immunocompetent mice (Grubor-Bauk et al., 2019); however, the contribution of NS1-specific antibodies in controlling the viremia throughout the infection was not ruled out in that study. Furthermore,

the NS1 vaccine did not provide full protection for ZIKV-susceptible *Ifnar<sup>-/-</sup>* mice because most of the immunized mice did not survive the challenge (only about 20% survival rate) with ZIKV (Grubor-Bauk et al., 2019). Both studies have not yet determined whether NS1-specific immune responses are sufficient for the prevention of ZIKV from transmission through placenta to fetuses and consequent damage.

We have made a vaccine that expressed Ub and rearranged ZIKV NS3 protein to generate CTLs without ADE-mediating antibodies. This NS3 design is expected to lead to rapid degradation in the proteasome. Our western blot result showed negligible amounts of the rearranged NS3 protein in the cells transfected with the plasmid expressing the NS3. In contrast, large amounts of NS3 can be seen with a proteasome inhibitor, indicating that the Ub/rearranged NS3 protein is rapidly degraded in the proteasome. We did not expect that large numbers of NS3-specific antibodies would be induced due to a lack of intact NS3, which was confirmed by ELISA. There was not much concern that even small numbers of antibodies to NS3 were induced, as NS3 is not on ZIKV virion surface. Indeed, sera from mice immunized with our vaccine did not show any ADE activity. As expected, the vaccine induced a strong NS3-specific CTL response. This is most likely due to the use of Ub upstream of the rearranged NS3 sequence, which promotes protein degradation in the proteasome, where antigenic peptides are loaded on MHC class I to induce CTL response (Rodriguez et al., 1997). Furthermore, we rearranged the NS3 sequence to avoid potential harmful effects of an intact NS3 protein. Although transfection of 293T cells with a plasmid expressing non-rearranged ZIKV NS3 did not show any obvious toxic effects, this strategy could be used to construct vaccines expressing viral proteins with harmful activity such as an oncoprotein HPV E6/7.

This study demonstrated that a ZIKV vaccine inducing NS3-specific CTLs provided full protection against ZIKV challenge, particularly against fetal damage in pregnant mice. Our data suggest that the CTLs controlled the virus infection in the placenta so that virus-induced inflammation was greatly reduced and fetal damage was prevented. Our data indicate that CTLs alone are sufficient to provide protection against viral infection.

It is believed that neutralizing antibodies and CTLs were needed to clear viruses (Grifoni et al., 2017; Hassert et al., 2019; Osuna and Whitney, 2017; Regla-Nava et al., 2018). The most devastating consequence of ZIKV infection is congenital syndrome, which may develop in DENV-endemic countries. DENV and ZIKV are very similar and share CTL epitopes, as determined in *Ifnar1<sup>-/-</sup>* HLA-transgenic mice (Wen et al., 2017b). It has been shown that DENV-specific antibodies enhance transmission of ZIKV from mother to fetuses (Brown et al., 2019; Langerak et al., 2019; Rathore et al., 2019) and that these antibodies cross-reacted with ZIKV but did not neutralize the virus (Bardina et al., 2017; Dejnirattisai et al., 2016). The passive transfer experiments showed no role for DENV-immune sera in the protection against ZIKV challenge (Grifoni et al., 2017; Regla-Nava et al., 2018; Wen et al., 2017a). However, it has been shown that preexisting high-antibody titers to DENV were associated with a reduced risk of ZIKV infection and symptoms in humans (Rodriguez-Barraquer et al., 2019). Thus, it is unclear if the DENV-specific antibodies promote or prevent ZIKV infections (cross-neutralizing antibodies, if present, may prevent ZIKV infection). It is unknown if DENV-specific CTLs are sufficient in protecting against ZIKV infection.

In mice, both CD8<sup>+</sup> T cell depletion and adaptive transfer of CD8<sup>+</sup> T cell experiments demonstrated that the ZIKV protection was provided principally by DENV-specific CTLs (Grubor-Bauk et al., 2019; Huang et al., 2017; Elong Ngonu and Shresta, 2019; Regla-Nava et al., 2018; Wen et al., 2017a). However, it is unclear if DENV immunity prevents or reduces fetal ZIKV infection in humans. It has been shown that there is an 11%–13% risk of microcephaly born to Brazilian women infected with ZIKV during pregnancy, particularly in the first trimester of pregnancy (de Araújo et al., 2018; Brady et al., 2019; Johansson et al., 2016; Regla-Nava et al., 2018). A recent study showed that the ZIKV-induced microcephaly occurred in the DENV-immune mothers (Reynolds et al., 2020), suggesting that T cell immunity does not provide sufficient cross-protection among ZIKV and DENV serotypes. The protection may be dependent on the numbers of cross-reacting CTLs and neutralizing antibodies (if any) at the time of ZIKV infection. It is likely that DENV-immune individuals presenting large numbers of CTLs cross-reacting with ZIKV and high titers of neutralizing antibodies cross-reacting with ZIKV will be protected, whereas those with small numbers of CTLs and low titers of neutralizing antibodies cross-reacting with ZIKV will suffer from congenital syndromes such as microcephaly. Thus, it is safe to design a vaccine expressing NS3 from ZIKV and DENV to induce a large number of memory CTLs to prevent against their infections.

Vaccines for humans usually induce neutralizing antibodies, an expected goal for many vaccines against infectious agents. However, these vaccines also induce non-neutralizing antibodies. Non-neutralizing antibodies may also protect the host from diseases such as HIV, CMV, and influenza (Alter and Barouch, 2018; Nelson et al., 2018; Sutton et al., 2017; Winarski et al., 2019) via antibody-mediated cell cytotoxicity, antibody-dependent cell phagocytosis, and antibody-dependent complement-mediated lysis (Jegaskanda, 2018; Jegaskanda et al., 2013; van der Lubbe et al., 2018; Winarski et al., 2019). The non-neutralizing antibodies, however, can augment the infection of viruses such as influenza virus and coronaviruses in addition to DENV and ZIKV (Bardina et al., 2017; Shim et al., 2019; Vanderven et al., 2018; Wang et al., 2014). The most alarming concern is that the DENV vaccine, Dengvaxia, has led to more severe consequences in individuals without DENV infection than in those with prior DENV infection, most likely due to ADE (Halstead, 2017; Martínez-Vega et al., 2017). Furthermore, non-neutralizing or suboptimal antibodies may also cause tissue damage, as anti-SARS-CoV full-length spike IgG antibodies induced by a vaccine have caused acute lung inflammation via activating macrophages by Fc $\gamma$  receptor (Fc $\gamma$ R) (Liu et al., 2019). This raised concerns if anti-SARS-CoV-2 full-length spike protein induced by vaccines would enhance lung inflammation when the neutralizing antibodies wane over time. Our study demonstrates that a vaccine inducing solely CTLs can fully protect from viral infection, which provides a strategy for developing safe and effective vaccines for viral infections without inducing antibody-mediated pathology.

## STAR★METHODS

### RESOURCE AVAILABILITY

**Lead contact**—Further information and requests for the supporting data, resources, and reagents should be directed to and will be fulfilled upon request by the lead contact, Liang Qiao (lqiao@luc.edu).

**Materials availability**—Plasmids generated in this study are stored in the lab of L.Q. and are available upon request. No samples have been submitted/banked in a public facility.

**Data and code availability**—This study did not generate datasets/code.

### EXPERIMENTAL MODEL AND SUBJECT DETAILS

**Mice**—Four-to-10-week-old female BALB/c mice and 4-6-week-old male and female interferon- $\alpha/\beta$  receptor (IFNAR)-deficient (*Ifnar1*<sup>-/-</sup>) mice were used in the studies. The animal studies were performed in strict accordance with the recommendations in the Guide for the Care and Use of Laboratory Animals, National Research Council (National Academy of Sciences, 2011). The protocols were approved by the Institutional Animal Care and Use Committee of the New York Blood Center (Permit Numbers: 344 and 345).

**Cell lines**—Vero E6, K562 and 293T cells were purchased from ATCC. The Vero E6 were cultured with DMEM containing 1% carboxymethyl cellulose and 2% FBS, at 37°C with 5% CO<sub>2</sub>. The 293T and K562 cells were cultured with DMEM containing 10% FBS at 37°C with 5% CO<sub>2</sub>.

**Viruses**—Zika virus (human strain R103451 (2015/Honduras)) and Zika virus (human strain PAN2016 (2016/Panama)) were from BEI.

### METHOD DETAILS

**Construction of the vaccine plasmid**—ZIKV NS3 sequence was rearranged and a ubiquitin monomer sequence was added to the front of the rearranged NS3 (see Results section). A Kozak sequence was placed ahead of the Ub/NS3 open reading frame to ensure efficient transcription of the plasmid. Upstream the Kozak sequence, linker DNA as well as an EcoRI restriction site was placed to facilitate proper cloning of the gene segment into the vector of interest. Downstream the rearranged Ub/NS3 gene sequence, a stop codon was placed along with linker DNA and a NotI restriction site. This nucleotide sequence was ordered through the GeneArt program (Thermo Fisher Scientific). The NS3 gene was delivered in a proprietary Thermo Fisher Scientific vector in a lyophilized form. Plasmid DNA was resuspended in Molecular Biology Grade water (Fisher Scientific) to a concentration of approximately 200 ng/uL. DNA was digested with FastDigest (FD) EcoRI and NotI for 15 min in a 37°C heat block. The digested DNA was then loaded directly onto a 1% Agarose gel and allowed to run for 40 min at 80V. The 2.2 kb Ub/NS3 DNA was exposed to 440 nm UV light in the imaging room and excised. The gel slice was placed into a clear, 1.5 mL microcentrifuge tube and the purified DNA was extracted using a QIAquick Gel Extraction Kit (QIAGEN). This gene fragment was stored in a -20°C freezer as the

pVAX1 vector (Thermo Fisher Scientific) was digested with FD EcoRI and FDNotI, run on a gel, and extracted using the same kit. The Ub/NS3 gene fragment was ligated using a 3:1 ratio of insert DNA (Ub/NS3) to vector DNA (pVAX1) at room temperature in the presence of T4 DNA ligase.

**Bacterial transformation**—Previously made Chemically Competent DH5 $\alpha$  *E. coli* was removed from  $-80^{\circ}\text{C}$  freezer and thawed on ice for 25 min. Ligated Ub/NS3/pVAX1 was introduced to the *E. coli* and remained on ice for 30 more min. Heat shock transformation occurred by placing the tube into a  $42^{\circ}\text{C}$  heat block for 45 s and back on ice for 2 min. 1 mL of SOC media was added to the *E. coli* and was grown in a shaking incubator at  $37^{\circ}\text{C}$  for 45 min. The *E. coli* was then spun down at 9,000 rpm for 2 min, resuspended in 200  $\mu\text{L}$  SOC media, and streaked on an LB Kanamycin (Kan<sup>+</sup>) plate. Once dry, the plate was inverted and incubated overnight at  $37^{\circ}\text{C}$ . Colonies from the plate were inoculated into 2 mL LB Kan<sup>+</sup> media, and a Miniprep was conducted using a QIAprep Spin Miniprep Kit according to the manufacturer's instructions (QIAGEN). Plasmid was subsequently re-digested with FD EcoRI and NotI. Upon observance of correct band digestion, the plasmid was sent out for sequencing (ACGT, Inc) for confirmation of correct insertion.

**Plasmid transfection**—293T cells were cultured in Dulbecco's Modified Eagle Medium (DMEM) with 10% Fetal Bovine Serum (FBS) and 1% Penicillin/Streptomycin. Cells were split upon reaching 90% confluence (every 2-3 days). Upon sufficient generation of 293T cells, 10  $\mu\text{g}$  of Ub/NS3/pVAX1 plasmid was transfected using PEI transfection reagent overnight. Media was removed the next morning and cells were cultured in DMEM. For subsequent experiments using proteasome inhibitor, MG132 was added to cell culture medium in a 1:1,000 ratio overnight at either 12, 36, or 60 h after transfection.

**qRT-PCR**—After 293T cells were transfected as described above, purification of total RNA was conducted using a RNeasy Mini Kit according to the manufacturer's instructions (QIAGEN). First-Strand cDNA was then synthesized using a GoScript Reverse Transcription System according to the manufacturer's instructions (Promega). In a PCR tube, the RNA harvested from transfected 293T cells was incubated with NS3-specific primers along with GAPDH primers (negative control) in a heat block at  $70^{\circ}\text{C}$  for 5 min. Tubes were immediately placed on ice for 10 min. RNA/primer mix was mixed with GoScript Reverse Transcription mix in a 3:1 ratio for each reaction. Tubes were placed on a heat block at  $25^{\circ}\text{C}$  for 5 min, then placed on a heat block at  $42^{\circ}\text{C}$  for 1 h. Reverse transcriptase was inactivated by placing tubes in a heat block at  $70^{\circ}\text{C}$  for 15 min. The qRT-PCR was conducted using iTaq Universal SYBR Green Supermix (Bio-Rad) using NS3-specific primers as well as GAPDH specific primers (negative control). Fold induction was measured as  $2^{-\text{C}_T}$ .

**Western blot**—293T cells were cultured, transfected, and treated with proteasome inhibitor as described above. After overnight treatment with 50 mM MG132, 293T cells were treated with 0.25% trypsin for 5 min at  $37^{\circ}\text{C}$  in 5%  $\text{CO}_2$ . 293T cells were resuspended in DMEM, centrifuged at 1,200 rpm for 5 min, and cell pellets were resuspended in RIPA buffer with freshly added proteinase inhibitor. Total protein concentration was calculated via

Bradford Assay (Bio-Rad) and 6x SDS Loading Buffer was added to 20 µg of total protein. Protein was denatured at 100°C for 10 min and then placed on ice for 2-3 min. Proteins were run on a 12% polyacrylamide gel for 20 min at 80V and for 40 minutes at 120V, or until the dye line reached the bottom of the gel. Bands from the polyacrylamide gel were transferred to a nitrocellulose membrane using an iBlot Gel Transfer Device (Thermo Fisher Scientific). Membrane was blocked in 5% blocking buffer (5% non-fat milk in PBS) for 1 h. Membrane was washed in PBS-Tween 20 (PBS-T) and blocked in 5% blocking buffer containing a 1:1,000 dilution of anti-ZIKV NS3 antibody (Genetex) overnight. The next day, the membrane was washed with PBS-T for 20 min, and the membrane was blocked in 5% blocking buffer with secondary horseradish peroxidase (HRP)-conjugated goat anti-rabbit antibody for 1 h. Membrane was washed in PBS-T for 20 min, and then exposed to 10 mL Chemiluminescent substrate for 3 min devoid of light. Proteins were visualized using a FluorChem E system (ProteinSimple).

**Immunization of mice with vaccines**—ZIKV E ectodomain, EDI/EDII peptides, and TCI-DNA vaccines were used to immunize mice as previously described (Tai et al., 2019a). Briefly, groups of six female BALB/c (4-6-week old), female *Ifnar1*<sup>-/-</sup> (4-week old), or mixed-sex *Ifnar1*<sup>-/-</sup> (3 female and 3 male, 5-6-week old) mice were intramuscularly (i.m.) immunized with ZIKV E ectodomain (Aviva Systems Biology; 10 µg/mouse) or EDI/EDII peptides (50 µg/mouse) in the presence of Alum (500 µg/mouse) and MPL (10 µg/mouse) adjuvants (InvivoGen), or with TCI-DNA (10 µg/mouse) in the presence of Imiquimod adjuvant (20 µg/mouse, InvivoGen). Mice injected with PBS were included as a control. The immunized mice were boosted once at three weeks, and sera were collected 10 days post-last dose to detect IgG antibodies, neutralizing antibodies, and/or ADE. The immunized mice were further processed for subsequent challenge experiments as described below. In two additional experiments, groups of five to six male or female BALB/c mice (6-10-week old) were immunized with TCI-DNA (10 µg/mouse) or PBS (control), depleted for CD4<sup>+</sup> or CD8<sup>+</sup>T cells, and subjected to subsequent challenge experiments, as described in Figure S2.

**ELISA**—ZIKV-, E-, or NS3-specific IgG antibodies were detected by ELISA in the immunized mouse sera (Du et al., 2016; Tai et al., 2019a). Briefly, ELISA plates were pre-coated with ZIKV E ectodomain (1 µg/ml), NS3 peptides, or ZIKV (human strain R103451 (2015/Honduras))-infected Vero E6 cell lysates at 4°C overnight and blocked with PBS-T containing 2% non-fat milk at 37°C for 2 h. After three washes with PBS-T, the plates were then sequentially incubated at 37°C for 1 h with serially diluted mouse sera and HRP-conjugated anti-mouse IgG-Fab antibody (1:5,000, Sigma). The substrate 3,3',5,5'-tetramethylbenzidine (TMB) (Sigma) was added to the plates, and the reaction was stopped after addition of 1N H<sub>2</sub>SO<sub>4</sub>. Absorbance at 450 nm (A<sub>450</sub>) was measured using ELISA plate reader (Tecan).

**In vitro ADE assay**—ADE potentially induced by immunized mouse serum antibodies was measured in K562 cells using a flow cytometry-based assay (de Alwis et al., 2014). Briefly, 100 PFU of ZIKV (strain R103451) was mixed with sera at 4-fold serial dilutions, and incubated at 37°C for 1 h. The virus-serum mixture was then added to K562 cells (5 × 10<sup>4</sup>/well), and incubated at 37°C for 2 h in DMEM containing 10% FBS and 1% Penicillin/

Streptomycin, followed by washing the cells with fresh DMEM, and culturing them for 3 days. The cells were then fixed, permeabilized, and sequentially stained with mouse anti-flavivirus 4G2 monoclonal antibody (mAb, 2 µg/ml) and FITC-conjugated anti-mouse antibody (1:100, Biolegend). The percent of infected cells was calculated based on the fluorescence signals in the presence or absence of serially diluted mouse sera.

**ZIKV challenge studies and evaluation of vaccine efficacy in mice**—The following five experiments were designed to evaluate the efficacy of vaccines in the immunized mice (Figure S2; Richner et al., 2017a; Tai et al., 2019a). (1) At 13 days post-last dose of E ectodomain, EDI/EDII peptides, TCI-DNA vaccine, or PBS control, *Ifnar1*<sup>-/-</sup> mice (male and female) were challenged (I.P.) with ZIKV (human strain R103451; 10<sup>3</sup> PFU; 200 µl/mouse), and investigated for survival and weight daily for 14 days. (2) Immunized *Ifnar1*<sup>-/-</sup> mice were challenged (I.P.) with ZIKV (human strain PAN2016 (2016/Panama), 10<sup>3</sup> PFU/mouse; 200 µl/mouse) as in (1), and 6 days later, sera and tissues were collected for detection of viral titers by plaque-forming assay (described below). (3) Ten days post-last dose of E ectodomain, EDI/EDII peptides, TCI-DNA, or PBS control, female BALB/c and *Ifnar1*<sup>-/-</sup> mice were mated with respective naive male mice for pregnancy. The pregnant mice (E5-E7 for BALB/c, and E10-E12 for *Ifnar1*<sup>-/-</sup> mice) were challenged (I.P.) with ZIKV (strain R103451, 2 × 10<sup>5</sup> PFU/mouse for BALB/c, and 10<sup>4</sup> PFU/mouse for *Ifnar1*<sup>-/-</sup> mice). Six days p.i., sera and tissues of adult mice, as well as placenta, amniotic fluid, and/or fetal brain, were collected for detection of viral titers, and uteri and/or fetuses were collected for analysis of morphological changes. (4) Ten days post-last dose of TCI-DNA or PBS control, male and female BALB/c mice were injected (I.P.) with or without anti-mouse-CD4 (IgG2b) mAb, anti-mouse-CD8a (IgG2b) mAb (200 µg/mouse) or IgG2b isotype control mAb (Bio X Cell) at -2, -1, and 1 days post-ZIKV challenge, and the mice were (I.P.) challenged with ZIKV (strain R103451, 2 × 10<sup>5</sup> PFU/mouse). The challenged mice were sacrificed at 3 days p.i., peripheral blood cells and splenocytes were evaluated for CD4<sup>+</sup> and CD8<sup>+</sup> T cell depletion by flow cytometry analysis, and sera and tissues were examined for viral titers by plaque-forming assay. (5) Ten days post-last dose of TCI-DNA or PBS control, female BALB/c mice were mated with naive male BALB/c mice for pregnancy. The pregnant mice (E10-E12) were injected (I.P.) with or without anti-CD8a (IgG2a) mAb (200 µg/mouse, for TCI-DNA) or IgG2a isotype control mAb (for PBS) (Bio X Cell) at -2, -1, and 3 days post-ZIKV challenge, and peripheral blood cells (collected at 6 h before infection and 3 days p.i.) and splenocytes (collected at 6 days p.i.) were evaluated for CD8<sup>+</sup> T cell depletion by flow cytometry analysis (Zhong et al., 2017). The pregnant mice with or without CD8<sup>+</sup> T cell depletion were then (I.P.) challenged with ZIKV (strain R103451, 2 × 10<sup>5</sup> PFU/mouse). Sera (collected 3 and 6 days p.i.), amniotic fluid, and tissues (placenta and fetal brain) (collected 6 days p.i.) were detected for viral titers by plaque-forming assay, fetuses and uteri (collected 6 days p.i.) were observed for morphological analysis, and splenocytes (collected 6 days p.i.) were used to detect ZIKV-specific CD8<sup>+</sup> T cell responses by flow cytometry analysis, as described below. For all groups in (1) to (5), the challenged mice with greater than 25% weight loss and significant clinical symptoms were humanely euthanized. For all BALB/c mice with ZIKV challenge, an anti-IFNAR1 blocking mAb (MAR1-5A3, 2 mg/mouse; Leinco) were injected into mice 1 day before ZIKV infection.

**Plaque reduction neutralization test (PRNT) and plaque-forming assay—PRNT**

and plaque-forming assays were performed to detect neutralizing antibodies in the immunized mouse sera and viral titers in the challenged mice, respectively (Tai et al., 2018, 2019a, 2019b). For PRNT assay, ZIKV (strain R103451, 100 PFU/mouse) was incubated with 2-fold serially diluted mouse sera at 37°C for 1.5 h, which was added to Vero E6 cells and culture of the cells at 37°C for 1 h. The cells were further overlaid with DMEM containing 1% carboxymethyl cellulose and 2% FBS, and cultured at 37°C for 4-5 days, followed by staining with crystal violet (0.5%). 50% PRNT titers (PRNT<sub>50</sub>) were calculated based on 2-fold serial dilutions of individual mouse serum at 50% plaque reduction using the CalcuSyn computer program (Chou, 2006; Tai et al., 2019a). For plaque-forming assay, sera, amniotic fluid, and tissue lysates of ZIKV-challenged mice were serially diluted and transferred to Vero E6 cells, followed by similar procedures as described above. Viral titers were calculated as PFU/g or PFU/ml of test samples.

**Immunofluorescence staining—**

This was performed as previously described (Tai et al., 2019b). Briefly, maternal placental tissues were harvested from the challenged pregnant *Ifnar1<sup>-/-</sup>* mice, and fixed in 4% paraformaldehyde (MilliporeSigma), which were further embedded in paraffin and sectioned. For vimentin staining, the deparaffinized tissue slides were blocked with 2% BSA (MilliporeSigma) for 30 min at room temperature, and then sequentially incubated with ZIKV EDIII-specific human mAb (ZV-64, 1:200, Absolute Antibody) and rabbit anti-vimentin antibody (1:300, Abcam). For caspase-3 staining, the tissue slides were fixed and permeated with FIX and PERM Cell Permeabilization Kit (Thermo Fisher Scientific), before being blocked as described above and incubated sequentially with ZV-64 and rabbit anti-active caspase-3 antibody (1:200, Abcam). The slides were washed with PBS, and incubated for 1 h at room temperature with anti-human FITC (1:300, Sigma; for ZIKV)- or anti-rabbit Alexa Fluor® 647 (1:300, Abcam; for vimentin and caspase-3)-conjugated antibodies, which were counter-stained for nuclei for 5 min with DAPI (4',6-diamidino-2-phenylindole, 300 nM; Thermo Fisher Scientific), and mounted in a Mounting Medium (VectaMount Permanent; Vector Laboratories). The stained slides were imaged on a confocal microscope (Zeiss LSM 880), and prepared for images using ZEN software. The fluorescence signals were quantified by ImageJ software for relative intensity (particle analysis) as described previously (Tai et al., 2019b).

**Detection of inflammatory cytokines and chemokines—**

Maternal placental tissues collected from the challenged pregnant *Ifnar1<sup>-/-</sup>* mice were measured for inflammatory cytokines and chemokines using Mouse Inflammatory Cytokines Multi-Analyte ELISArray Kit and Mouse Common Chemokines Multi-Analyte ELISArray Kit (QIAGEN) (Tai et al., 2019b). Briefly, ELISA plates were pre-coated with cytokine or chemokine capture antibodies, followed by incubation with tissue lysates for 2 h at room temperature. After three washes, the plates were sequentially incubated with detection antibody for 1 h, and Avidin-HRP conjugates for 30 min at room temperature, followed by incubation with development and stop solutions, respectively. A450 value was measured using ELISA plate reader (Tecan).

**Flow cytometry**—Flow cytometry analysis was performed to evaluate CD4<sup>+</sup> and CD8<sup>+</sup> T cell depletion and ZIKV-specific CD8<sup>+</sup> T cell responses in the challenged mice (Guerrero et al., 1986; Zhang et al., 2016). For analysis of CD4<sup>+</sup> and CD8<sup>+</sup> depletion in whole blood and splenocytes, peripheral blood cells and splenocytes were treated with 1 × Red Blood Cell Lysis Buffer (Biolegend), and stained with FITC-anti-mouse CD4 or PerCP-Cy5.5-anti-mouse CD8 antibody (BD Biosciences), followed by flow cytometry analysis using BD LSRFortessa 4 system. For analysis of ZIKV-specific CD8<sup>+</sup> T cell responses, the above-treated splenocytes (2 × 10<sup>6</sup> cells/well) were incubated with ZIKV NS3 overlapping peptides (0.25 nM/peptide, final concentration 5 µg/ml) in the presence of 5 µg/ml brefeldin A (Biolegend), and cultured at 37°C for 5 h. After stimulation, the cells were washed with PBS and stained for surface marker using PerCP/Cy5.5 anti-mouse CD8a. After fixation and permeabilization, the cells were stained for intracellular markers using FITC-anti-mouse IL-2, PE-anti-mouse IFN-γ, and Brilliant Violet 421-anti-mouse TNF-α antibodies (BD Biosciences), followed by analysis using flow cytometry as described above.

## QUANTIFICATION AND STATISTICAL ANALYSIS

All values are expressed as mean with standard error (SEM). Statistical significance of antibody titers among different groups was calculated using the Mann-Whitney test. Statistical significance of viral titers, fluorescence intensity, cytokines and chemokines, as well as CD8<sup>+</sup> T cell responses, among various groups was calculated using a Student's two-tailed t test. Statistical significance of survival rates among different groups was calculated using the Log-Rank test. The data were analyzed using GraphPad Prism Statistical Software. \*, \*\* and \*\*\* indicate  $p < 0.05$ ,  $p < 0.01$ , and  $p < 0.001$ , respectively.

## Supplementary Material

Refer to Web version on PubMed Central for supplementary material.

## ACKNOWLEDGMENTS

This research was supported by NIH grant R21AI137790 to L.D., NIH grant R21AI140210 to L.Q., and intramural fund of the New York Blood Center (NYB616 and NYB673). ZIKV strains (R103451 and PAN2016) were obtained from BEI Resources.

## REFERENCES

- Abbink P, Larocca RA, De La Barrera RA, Bricault CA, Moseley ET, Boyd M, Kirilova M, Li Z, Ng'ang'a D, Nanayakkara O, et al. (2016). Protective efficacy of multiple vaccine platforms against Zika virus challenge in rhesus monkeys. *Science* 353, 1129–1132. [PubMed: 27492477]
- Abbink P, Larocca RA, Visitsunthorn K, Boyd M, De La Barrera RA, Gromowski GD, Kirilova M, Peterson R, Li Z, Nanayakkara O, et al. (2017). Durability and correlates of vaccine protection against Zika virus in rhesus monkeys. *Sci. Transl. Med* 9, eaao4163. [PubMed: 29237759]
- Alter G, and Barouch D (2018). Immune Correlate-Guided HIV Vaccine Design. *Cell Host Microbe* 24, 25–33. [PubMed: 30001521]
- Barba-Spaeth G, Dejnirattisai W, Rouvinski A, Vaney MC, Medits I, Sharma A, Simon-Lorière E, Sakuntabhai A, Cao-Lormeau VM, Haouz A, et al. (2016). Structural basis of potent Zika-dengue virus antibody cross-neutralization. *Nature* 536, 48–53. [PubMed: 27338953]

- Barbosa M, Joshi RS, Garg P, Martin-Trujillo A, Patel N, Jadhav B, Watson CT, Gibson W, Chetnik K, Tessereau C, et al. (2018). Identification of rare de novo epigenetic variations in congenital disorders. *Nat. Commun* 9, 2064. [PubMed: 29802345]
- Bardina SV, Bunduc P, Tripathi S, Duehr J, Frere JJ, Brown JA, Nachbagauer R, Foster GA, Krysztof D, Tortorella D, et al. (2017). Enhancement of Zika virus pathogenesis by preexisting antinflavivirus immunity. *Science* 356, 175–180. [PubMed: 28360135]
- Brady OJ, Osgood-Zimmerman A, Kassebaum NJ, Ray SE, de Araújo VEM, da Nóbrega AA, Frutuoso LCV, Lecca RCR, Stevens A, Zoca de Oliveira B, et al. (2019). The association between Zika virus infection and microcephaly in Brazil 2015-2017: An observational analysis of over 4 million births. *PLoS Med.* 16, e1002755. [PubMed: 30835728]
- Brasil P, Pereira JP Jr., Moreira ME, Ribeiro Nogueira RM, Damasceno L, Wakimoto M, Rabello RS, Valderramos SG, Halai UA, Salles TS, et al. (2016). Zika virus infection in pregnant women in Rio de Janeiro. *N. Engl. J. Med* 375, 2321–2334. [PubMed: 26943629]
- Brault AC, Domi A, McDonald EM, Talmi-Frank D, McCurley N, Basu R, Robinson HL, Hellerstein M, Duggal NK, Bowen RA, and Guirakhoo F (2017). A Zika vaccine targeting NS1 protein protects immunocompetent adult mice in a lethal challenge model. *Sci. Rep* 7, 14769. [PubMed: 29116169]
- Brown JA, Singh G, Acklin JA, Lee S, Duehr JE, Chokola AN, Frere JJ, Hoffman KW, Foster GA, Krysztof D, et al. (2019). Dengue virus immunity increases Zika virus-induced damage during pregnancy. *Immunity* 50, 751–762.e5. [PubMed: 30737148]
- Bullard BL, Corder BN, Gorman MJ, Diamond MS, and Weaver EA (2018). Efficacy of a T Cell-biased adenovirus vector as a Zika virus vaccine. *Sci. Rep* 8, 18017. [PubMed: 30573745]
- Cao-Lormeau VM, Blake A, Mons S, Lastère S, Roche C, Vanhomwegen J, Dub T, Baudouin L, Teissier A, Larre P, et al. (2016). Guillain-Barré Syndrome outbreak associated with Zika virus infection in French Polynesia: a case-control study. *Lancet* 387, 1531–1539. [PubMed: 26948433]
- Chou TC (2006). Theoretical basis, experimental design, and computerized simulation of synergism and antagonism in drug combination studies. *Pharmacol. Rev* 58, 621–681. [PubMed: 16968952]
- Dans AL, Dans LF, Lansang MAD, Silvestre MAA, and Guyatt GH (2018). Controversy and debate on dengue vaccine series-paper 1: review of a licensed dengue vaccine: inappropriate subgroup analyses and selective reporting may cause harm in mass vaccination programs. *J. Clin. Epidemiol* 95, 137–139. [PubMed: 29180056]
- Dar H, Zaheer T, Rehman MT, Ali A, Javed A, Khan GA, Babar MM, and Waheed Y (2016). Prediction of promiscuous T-cell epitopes in the Zika virus polyprotein: An in silico approach. *Asian Pac. J. Trop. Med* 9, 844–850. [PubMed: 27633296]
- de Alwis R, Williams KL, Schmid MA, Lai CY, Patel B, Smith SA, Crowe JE, Wang WK, Harris E, and de Silva AM (2014). Dengue viruses are enhanced by distinct populations of serotype cross-reactive antibodies in human immune sera. *PLoS Pathog.* 10, e1004386. [PubMed: 25275316]
- de Araújo TVB, Ximenes RAA, Miranda-Filho DB, Souza WV, Montarroyos UR, de Melo APL, Valongueiro S, de Albuquerque MFPM, Braga C, Filho SPB, et al. ; investigators from the Microcephaly Epidemic Research Group; Brazilian Ministry of Health; Pan American Health Organization; Instituto de Medicina Integral Professor Fernando Figueira; State Health Department of Pernambuco (2018). Association between microcephaly, Zika virus infection, and other risk factors in Brazil: final report of a case-control study. *Lancet Infect. Dis* 18, 328–336. [PubMed: 29242091]
- Dejnirattisai W, Supasa P, Wongwiwat W, Rouvinski A, Barba-Spaeth G, Duangchinda T, Sakuntabhai A, Cao-Lormeau VM, Malasit P, Rey FA, et al. (2016). Dengue virus sero-cross-reactivity drives antibody-dependent enhancement of infection with Zika virus. *Nat. Immunol* 17, 1102–1108. [PubMed: 27339099]
- Delgado FG, Torres KI, Castellanos JE, Romero-Sánchez C, Simon-Lorière E, Sakuntabhai A, and Roth C (2018). Improved Immune Responses Against Zika Virus After Sequential Dengue and Zika Virus Infection in Humans. *Viruses* 10, 480.
- Dowd KA, Ko SY, Morabito KM, Yang ES, Pelc RS, DeMaso CR, Castilho LR, Abbink P, Boyd M, Nityanandam R, et al. (2016). Rapid development of a DNA vaccine for Zika virus. *Science* 354, 237–240. [PubMed: 27708058]

- Driggers RW, Ho CY, Korhonen EM, Kuivanen S, Jääskeläinen AJ, Smura T, Rosenberg A, Hill DA, DeBiasi RL, Vezina G, et al. (2016). Zika virus infection with prolonged maternal viremia and fetal brain abnormalities. *N. Engl. J. Med* 374, 2142–2151. [PubMed: 27028667]
- Du L, Tai W, Yang Y, Zhao G, Zhu Q, Sun S, Liu C, Tao X, Tseng CK, Perlman S, et al. (2016). Introduction of neutralizing immunogenicity index to the rational design of MERS coronavirus subunit vaccines. *Nat. Commun* 7, 13473. [PubMed: 27874853]
- Edupuganti S, Natrajan MS, Roupheal N, Lai L, Xu Y, Feldhammer M, Hill C, Patel SM, Johnson SJ, Bower M, et al. (2017). Biphasic Zika Illness With Rash and Joint Pain. *Open Forum Infect. Dis* 4, ofx133. [PubMed: 28761900]
- El Sahly HM, Gorchakov R, Lai L, Natrajan MS, Patel SM, Atmar RL, Keitel WA, Hoft DF, Barrett J, Bailey J, et al. (2018). Clinical, Virologic, and Immunologic Characteristics of Zika Virus Infection in a Cohort of US Patients: Prolonged RNA Detection in Whole Blood. *Open Forum Infect. Dis* 6, ofy352. [PubMed: 30697574]
- Elong Ngono A, and Shresta S (2019). Cross-reactive T cell immunity to dengue and Zika viruses: New insights into vaccine development. *Front. Immunol* 10, 1316. [PubMed: 31244855]
- Fowler AM, Tang WW, Young MP, Mamidi A, Viramontes KM, McCauley MD, Carlin AF, Schooley RT, Swanstrom J, Baric RS, et al. (2018). Maternally acquired Zika antibodies enhance dengue disease severity in mice. *Cell Host Microbe*. 24, 743–750.e5. [PubMed: 30439343]
- Gao Y, Tai W, Wang N, Li X, Jiang S, Debnath AK, Du L, and Chen S (2019). Identification of novel natural products as effective and broad-spectrum anti-Zika virus inhibitors. *Viruses* 11, 1019.
- Gaudinski MR, Houser KV, Morabito KM, Hu Z, Yamshchikov G, Rothwell RS, Berkowitz N, Mendoza F, Saunders JG, Novik L, et al. ; VRC 319; VRC 320 study teams (2018). Safety, tolerability, and immunogenicity of two Zika virus DNA vaccine candidates in healthy adults: randomised, open-label, phase 1 clinical trials. *Lancet* 391, 552–562. [PubMed: 29217376]
- Gorman MJ, Caine EA, Zaitsev K, Begley MC, Weger-Lucarelli J, Uccellini MB, Tripathi S, Morrison J, Yount BL, Dinnon KH 3rd., et al. (2018). An Immunocompetent Mouse Model of Zika Virus Infection. *Cell Host Microbe* 23, 672–685.e6. [PubMed: 29746837]
- Griffin BD, Muthumani K, Warner BM, Majer A, Hagan M, Audet J, Stein DR, Ranadheera C, Racine T, De La Vega MA, et al. (2017). DNA vaccination protects mice against Zika virus-induced damage to the testes. *Nat. Commun* 8, 15743. [PubMed: 28589934]
- Grifoni A, Pham J, Sidney J, O'Rourke PH, Paul S, Peters B, Martini SR, de Silva AD, Ricciardi MJ, Magnani DM, et al. (2017). Prior dengue virus exposure shapes T cell immunity to Zika virus in humans. *J. Virol* 91, 1469–1470.
- Grubor-Bauk B, Wijesundara DK, Masavuli M, Abbink P, Peterson RL, Prow NA, Larocca RA, Mekonnen ZA, Shrestha A, Eyre NS, et al. (2019). NS1 DNA vaccination protects against Zika infection through T cell-mediated immunity in immunocompetent mice. *Sci. Adv* 5, eaax2388. [PubMed: 31844662]
- Guerrero JM, Goberna R, Molinero P, Jimenez J, and Calvo JR (1986). Interaction of a bovine thymic peptide extract with vasoactive intestinal peptide (VIP) receptors. *Biosci. Rep* 6, 579–584. [PubMed: 3021253]
- Halstead SB (2017). Dengvaxia sensitizes seronegatives to vaccine enhanced disease regardless of age. *Vaccine* 35, 6355–6358. [PubMed: 29029938]
- Hassert M, Harris MG, Brien JD, and Pinto AK (2019). Identification of protective CD8 T cell responses in a mouse model of Zikavirus infection. *Front. Immunol* 10, 1678. [PubMed: 31379867]
- He Z, Chen J, Zhu X, An S, Dong X, Yu J, Zhang S, Wu Y, Li G, Zhang Y, et al. (2018). NLRP3 inflammasome activation mediates Zika virus-associated inflammation. *J. Infect. Dis* 217, 1942–1951. [PubMed: 29518228]
- Herrera BB, Tsai WY, Brites C, Luz E, Pedroso C, Drexler JF, Wang WK, and Kanki PJ (2018a). T Cell Responses to Nonstructural Protein 3 Distinguish Infections by Dengue and Zika Viruses. *MBio* 9, e00755–18. [PubMed: 30087165]
- Herrera BB, Tsai WY, Chang CA, Hamel DJ, Wang WK, Lu Y, Mboup S, and Kanki PJ (2018b). Sustained Specific and Cross-Reactive T Cell Responses to Zika and Dengue Virus NS3 in West Africa. *J. Virol* 92, e01992–17. [PubMed: 29321308]

- Hilgenfeld R, Lei J, and Zhang L (2018). The structure of the Zika virus protease, NS2B/NS3(pro). *Adv. Exp. Med. Biol* 1062, 131–145. [PubMed: 29845530]
- Huang H, Li S, Zhang Y, Han X, Jia B, Liu H, Liu D, Tan S, Wang Q, Bi Y, et al. (2017). CD8+ T cell immune response in immunocompetent mice during Zika virus infection. *J. Virol* 91, e00900–e00917. [PubMed: 28835502]
- Jagger BW, Dowd KA, Chen RE, Desai P, Foreman B, Burgomaster KE, Himansu S, Kong WP, Graham BS, Pierson TC, and Diamond MS (2019). Protective efficacy of nucleic acid vaccines against transmission of Zika virus during pregnancy in mice. *J. Infect. Dis* 220, 1577–1588. [PubMed: 31260518]
- Jegaskanda S (2018). The Potential role of Fc-receptor functions in the development of a universal influenza vaccine. *Vaccines (Basel)* 6, 27.
- Jegaskanda S, Job ER, Kramski M, Laurie K, Isitman G, de Rose R, Winnall WR, Stratov I, Brooks AG, Reading PC, and Kent SJ (2013). Cross-reactive influenza-specific antibody-dependent cellular cytotoxicity antibodies in the absence of neutralizing antibodies. *J. Immunol* 190, 1837–1848. [PubMed: 23319732]
- Johansson MA, Mier-y-Teran-Romero L, Reefhuis J, Gilboa SM, and Hills SL (2016). Zika and the risk of microcephaly. *N. Engl. J. Med* 375, 1–4. [PubMed: 27222919]
- Kalayanarooj S (2011). Clinical manifestations and management of Dengue/DHF/DSS. *Trop. Med. Health* 39, 83–87.
- Khetarpal N, and Khanna I (2016). Dengue fever: Causes, complications, and vaccine strategies. *J. Immunol. Res* 2016, 6803098. [PubMed: 27525287]
- Langerak T, Mumtaz N, Tolck VI, van Gorp ECM, Martina BE, Rockx B, and Koopmans MPG (2019). The possible role of cross-reactive dengue virus antibodies in Zika virus pathogenesis. *PLoS Pathog.* 15, e1007640. [PubMed: 30998804]
- Larocca RA, Abbink P, Peron JP, Zanotto PM, Iampietro MJ, Badamchi-Zadeh A, Boyd M, Ng'ang'a D, Kirilova M, Nityanandam R, et al. (2016). Vaccine protection against Zika virus from Brazil. *Nature* 536, 474–478. [PubMed: 27355570]
- Larocca RA, Mendes EA, Abbink P, Peterson RL, Martinot AJ, Iampietro MJ, Kang ZH, Aid M, Kirilova M, Jacob-Dolan C, et al. (2019). Adenovirus vector-based vaccines confer maternal-fetal protection against Zika virus challenge in pregnant IFN- $\alpha$  mice. *Cell Host Microbe*. 26, 591–600.e4. [PubMed: 31668877]
- Lazear HM, and Diamond MS (2016). Zika virus: New clinical syndromes and its emergence in the Western Hemisphere. *J. Virol.* 90, 4864–4875. [PubMed: 26962217]
- Lei J, Hansen G, Nitsche C, Klein CD, Zhang L, and Hilgenfeld R (2016). Crystal structure of Zika virus NS2B-NS3 protease in complex with a boronate inhibitor. *Science* 353, 503–505. [PubMed: 27386922]
- Li Y, Phoo WW, Loh YR, Zhang Z, Ng EY, Wang W, Keller TH, Luo D, and Kang C (2017). Structural characterization of the linked NS2B-NS3 protease of Zika virus. *FEBS Lett.* 591, 2338–2347. [PubMed: 28675775]
- Liu L, Wei Q, Lin Q, Fang J, Wang H, Kwok H, Tang H, Nishiura K, Peng J, Tan Z, et al. (2019). Anti-spike IgG causes severe acute lung injury by skewing macrophage responses during acute SARS-CoV infection. *JCI Insight* 4, 4–123158.
- Martínez-Vega RA, Carrasquilla G, Luna E, and Ramos-Castañeda J (2017). ADE and dengue vaccination. *Vaccine* 35, 3910–3912. [PubMed: 28623027]
- Marzi A, Emanuel J, Callison J, McNally KL, Arndt N, Chadinha S, Martellaro C, Rosenke R, Scott DP, Safronetz D, et al. (2018). Lethal Zika virus disease models in young and older interferon alpha/beta receptor knock out mice. *Front. Cell. Infect. Microbiol* 8, 117. [PubMed: 29696134]
- Miner JJ, Cao B, Govero J, Smith AM, Fernandez E, Cabrera OH, Garber C, Noll M, Klein RS, Noguchi KK, et al. (2016). Zika virus infection during pregnancy in mice causes placental damage and fetal demise. *Cell* 165, 1081–1091. [PubMed: 27180225]
- Mirza MU, Rafique S, Ali A, Munir M, Ikram N, Manan A, Salo-Ahen OM, and Idrees M (2016). Towards peptide vaccines against Zika virus: Immunoinformatics combined with molecular dynamics simulations to predict antigenic epitopes of Zika viral proteins. *Sci. Rep* 6, 37313. [PubMed: 27934901]

- Morrison TE, and Diamond MS (2017). Animal models of Zika virus infection, pathogenesis, and immunity. *J. Virol* 91, e00009–17. [PubMed: 28148798]
- Murphy BR, and Whitehead SS (2011). Immune response to dengue virus and prospects for a vaccine. *Annu. Rev. Immunol* 29, 587–619. [PubMed: 21219187]
- National Academy of Sciences (2011). The National Academies Collection: Reports funded by National Institutes of Health. In *Guide for the Care and Use of Laboratory Animals*, Fletcher Cameron H. and Crossgrove Ruth, eds. (National Academies Press).
- Nelson CS, Huffman T, Jenks JA, Cisneros de la Rosa E, Xie G, Vandergrift N, Pass RF, Pollara J, and Permar SR (2018). HCMV glycoprotein B subunit vaccine efficacy mediated by nonneutralizing antibody effector functions. *Proc. Natl. Acad. Sci. USA* 115, 6267–6272. [PubMed: 29712861]
- Osuna CE, and Whitney JB (2017). Nonhuman primate models of Zikavirus infection, immunity, and therapeutic development. *J. Infect. Dis* 216, S928–S934. [PubMed: 29267926]
- Pardi N, Hogan MJ, Pelc RS, Muramatsu H, Andersen H, DeMaso CR, Dowd KA, Sutherland LL, Scearce RM, Parks R, et al. (2017). Zika virus protection by a single low-dose nucleoside-modified mRNA vaccination. *Nature* 543, 248–251. [PubMed: 28151488]
- Phoo WW, Li Y, Zhang Z, Lee MY, Loh YR, Tan YB, Ng EY, Lescar J, Kang C, and Luo D (2016). Structure of the NS2B-NS3 protease from Zika virus after self-cleavage. *Nat. Commun* 7, 13410. [PubMed: 27845325]
- Phoo WW, Zhang Z, Wirawan M, Chew EJC, Chew ABL, Kouretova J, Steinmetzer T, and Luo D (2018). Structures of Zika virus NS2B-NS3 protease in complex with peptidomimetic inhibitors. *Antiviral Res.* 160, 17–24. [PubMed: 30315877]
- Priyamvada L, Quicke KM, Hudson WH, Onlamoon N, Sewatanon J, Edupuganti S, Pattanapanyasat K, Chokephaibulkit K, Mulligan MJ, Wilson PC, et al. (2016). Human antibody responses after dengue virus infection are highly cross-reactive to Zika virus. *Proc. Natl. Acad. Sci. USA* 113, 7852–7857. [PubMed: 27354515]
- Rabelo K, Souza LJ, Salomão NG, Oliveira ERA, Sentinelli LP, Lacerda MS, Saraquino PB, Rosman FC, Basílio-de-Oliveira R, Carvalho JJ, and Paes MV (2018). Placental inflammation and fetal injury in a rare Zika case associated with Guillain-Barre Syndrome and abortion. *Front. Microbiol* 9, 1018. [PubMed: 29867903]
- Rathore APS, Saron WAA, Lim T, Jahan N, and St John AL (2019). Maternal immunity and antibodies to dengue virus promote infection and Zika virus-induced microcephaly in fetuses. *Sci. Adv* 5, eaav3208. [PubMed: 30820456]
- Regla-Nava JA, Elong Ngono A, Viramontes KM, Huynh AT, Wang YT, Nguyen AT, Salgado R, Mamidi A, Kim K, Diamond MS, and Shresta S (2018). Cross-reactive Dengue virus-specific CD8<sup>+</sup> T cells protect against Zika virus during pregnancy. *Nat. Commun* 9, 3042. [PubMed: 30072692]
- Reynolds CJ, Watber P, Santos CNO, Ribeiro DR, Alves JC, Fonseca ABL, Bispo AJB, Porto RLS, Bokea K, de Jesus AMR, et al. (2020). Strong CD4 T Cell Responses to Zika Virus Antigens in a Cohort of Dengue Virus Immune Mothers of Congenital Zika Virus Syndrome Infants. *Front. Immunol* 11, 185. [PubMed: 32132999]
- Richner JM, Himansu S, Dowd KA, Butler SL, Salazar V, Fox JM, Julander JG, Tang WW, Shresta S, Pierson TC, et al. (2017a). Modified mRNA vaccines protect against Zika virus infection. *Cell* 168, 1114–1125.e10. [PubMed: 28222903]
- Richner JM, Jagger BW, Shan C, Fontes CR, Dowd KA, Cao B, Himansu S, Caine EA, Nunes BT, Medeiros DBA, et al. (2017b). Vaccine mediated protection against Zika virus-induced congenital disease. *Cell* 170, 273–283.e12. [PubMed: 28708997]
- Rodriguez F, Zhang J, and Whitton JL (1997). DNA immunization: ubiquitination of a viral protein enhances cytotoxic T-lymphocyte induction and antiviral protection but abrogates antibody induction. *J. Virol* 71, 8497–8503. [PubMed: 9343207]
- Rodriguez-Barrquer I, Costa F, Nascimento EJM, Nery N, Castanha PMS, Sacramento GA, Cruz J, Carvalho M, De Olivera D, Hagan JE, et al. (2019). Impact of preexisting dengue immunity on Zika virus emergence in a dengue endemic region. *Science* 363, 607–610. [PubMed: 30733412]

- Sapparapu G, Fernandez E, Kose N, Bin Cao, Fox JM, Bombardi RG, Zhao H, Nelson CA, Bryan AL, Barnes T, et al. (2016). Neutralizing human antibodies prevent Zika virus replication and fetal disease in mice. *Nature* 540, 443–447. [PubMed: 27819683]
- Schrader EK, Harstad KG, and Matouschek A (2009). Targeting proteins for degradation. *Nat. Chem. Biol* 5, 815–822. [PubMed: 19841631]
- Screaton G, Mongkolsapaya J, Yacoub S, and Roberts C (2015). New insights into the immunopathology and control of dengue virus infection. *Nat. Rev. Immunol* 15, 745–759. [PubMed: 26603900]
- Shan C, Muruato AE, Nunes BT, Luo H, Xie X, Medeiros DBA, Wakamiya M, Tesh RB, Barrett AD, Wang T, et al. (2017). A live-attenuated Zika virus vaccine candidate induces sterilizing immunity in mouse models. *Nat. Med* 23, 763–767. [PubMed: 28394328]
- Shim BS, Kwon YC, Ricciardi MJ, Stone M, Otsuka Y, Berri F, Kwal JM, Magnani DM, Jackson CB, Richard AS, et al. (2019). Zika virus-immune plasmas from symptomatic and asymptomatic individuals enhance Zika pathogenesis in adult and pregnant mice. *MBio* 10, e00758–19. [PubMed: 31266863]
- Souza BS, Sampaio GL, Pereira CS, Campos GS, Sardi SI, Freitas LA, Figueira CP, Paredes BD, Nonaka CK, Azevedo CM, et al. (2016). Zika virus infection induces mitosis abnormalities and apoptotic cell death of human neural progenitor cells. *Sci. Rep* 6, 39775. [PubMed: 28008958]
- Sutton TC, Lamirande EW, Bock KW, Moore IN, Koudstaal W, Rehman M, Weverling GJ, Goudsmit J, and Subbarao K (2017). In vitro neutralization is not predictive of prophylactic efficacy of broadly neutralizing monoclonal antibodies CR6261 and CR9114 against lethal H2 influenza virus challenge in mice. *J. Virol* 91, e01603–e01617. [PubMed: 29046448]
- Tai W, He L, Wang Y, Sun S, Zhao G, Luo C, Li P, Zhao H, Fremont DH, Li F, et al. (2018). Critical neutralizing fragment of Zika virus EDIII elicits cross-neutralization and protection against divergent Zika viruses. *Emerg. Microbes Infect* 7, 7. [PubMed: 29362446]
- Tai W, Chen J, Zhao G, Geng Q, He L, Chen Y, Zhou Y, Li F, and Du L (2019a). Rational Design of Zika virus subunit vaccine with enhanced efficacy. *J. Virol* 93, e02187–18. [PubMed: 31189716]
- Tai W, Voronin D, Chen J, Bao W, Kessler DA, Shaz B, Jiang S, Yazdanbakhsh K, and Du L (2019b). Transfusion-transmitted Zika virus infection in pregnant mice leads to broad tissue tropism with severe placental damage and fetal demise. *Front. Microbiol* 10, 29. [PubMed: 30728813]
- Tebas P, Roberts CC, Muthumani K, Reuschel EL, Kudchodkar SB, Zaidi FI, White S, Khan AS, Racine T, Choi H, et al. (2017). Safety and immunogenicity of an anti-Zika virus DNA vaccine. *N. Engl. J. Med* Published online 10 4, 2017. 10.1056/nejmoa1708120.
- Tripathi S, Balasubramaniam VR, Brown JA, Mena I, Grant A, Bardina SV, Maringer K, Schwarz MC, Maestre AM, Sourisseau M, et al. (2017). A novel Zika virus mouse model reveals strain specific differences in virus pathogenesis and host inflammatory immune responses. *PLoS Pathog.* 13, e1006258. [PubMed: 28278235]
- van der Lubbe JEM, Huizingh J, Verspuij JWA, Tettero L, Schmit-Tillemans SPR, Mooij P, Mortier D, Koopman G, Bogers WMJM, Dekking L, et al. (2018). Mini-hemagglutinin vaccination induces cross-reactive antibodies in pre-exposed NHP that protect mice against lethal influenza challenge. *NPJ Vaccines* 3, 25. [PubMed: 29977611]
- Van Rompay KKA, Keesler RI, Ardeshir A, Watanabe J, Usachenko J, Singapuri A, Cruzen C, Bliss-Moreau E, Murphy AM, Yee JL, et al. (2019). DNA vaccination before conception protects Zika virus-exposed pregnant macaques against prolonged viremia and improves fetal outcomes. *Sci. Transl. Med* 11, eaay2736. [PubMed: 31852797]
- Vandervan HA, Wragg K, Ana-Sosa-Batiz F, Kristensen AB, Jegaskanda S, Wheatley AK, Wentworth D, Wines BD, Hogarth PM, Rockman S, and Kent SJ; INSIGHT FLU005 Pilot Study Writing Group (2018). Anti-influenza hyperimmune immunoglobulin enhances Fc-functional antibody immunity during human influenza infection. *J. Infect. Dis* 218, 1383–1393. [PubMed: 29860297]
- Waggoner JJ, Roupael N, Xu Y, Natrajan M, Lai L, Patel SM, Levit RD, Edupuganti S, and Mulligan MJ (2017). Pericarditis Associated With Acute Zika Virus Infection in a Returning Traveler. *Open Forum Infect. Dis* 4, ofx103. [PubMed: 28702470]

- Wang SF, Tseng SP, Yen CH, Yang JY, Tsao CH, Shen CW, Chen KH, Liu FT, Liu WT, Chen YM, and Huang JC (2014). Antibody-dependent SARS coronavirus infection is mediated by antibodies against spike proteins. *Biochem. Biophys. Res. Commun* 451, 208–214. [PubMed: 25073113]
- Wang X, Tai W, Zhang X, Zhou Y, Du L, and Shen C (2019). Effects of Adjuvants on the Immunogenicity and Efficacy of a Zika Virus Envelope Domain III Subunit Vaccine. *Vaccines (Basel)* 7, 161.
- Wen J, Elong Ngono A, Regla-Nava JA, Kim K, Gorman MJ, Diamond MS, and Shresta S (2017a). Dengue virus-reactive CD8<sup>+</sup> T cells mediate cross-protection against subsequent Zika virus challenge. *Nat. Commun* 8, 1459. [PubMed: 29129917]
- Wen J, Tang WW, Sheets N, Ellison J, Sette A, Kim K, and Shresta S (2017b). Identification of Zika virus epitopes reveals immunodominant and protective roles for dengue virus cross-reactive CD8<sup>+</sup> T cells. *Nat. Microbiol* 2, 17036. [PubMed: 28288094]
- Winarski KL, Tang J, Klenow L, Lee J, Coyle EM, Manischewitz J, Turner HL, Takeda K, Ward AB, Golding H, and Khurana S (2019). Antibody-dependent enhancement of influenza disease promoted by increase in hemagglutinin stem flexibility and virus fusion kinetics. *Proc. Natl. Acad. Sci. USA* 116, 15194–15199. [PubMed: 31296560]
- Yuan L, Huang XY, Liu ZY, Zhang F, Zhu XL, Yu JY, Ji X, Xu YP, Li G, Li C, et al. (2017). A single mutation in the prM protein of Zika virus contributes to fetal microcephaly. *Science* 358, 933–936. [PubMed: 28971967]
- Zhang N, Channappanavar R, Ma C, Wang L, Tang J, Garron T, Tao X, Tasneem S, Lu L, Tseng CT, et al. (2016). Identification of an ideal adjuvant for receptor-binding domain-based subunit vaccines against Middle East respiratory syndrome coronavirus. *Cell. Mol. Immunol* 13, 180–190. [PubMed: 25640653]
- Zhong Z, Zhai Y, Bu P, Shah S, and Qiao L (2017). Papilloma-pseudovirus eradicates intestinal tumours and triples the lifespan of Apc<sup>Min/+</sup> mice. *Nat. Commun* 8, 15004. [PubMed: 28397782]

**Highlights**

- Vaccine of modified ZIKV NS3 induces specific CTLs with little antibody response
- The vaccine fully protects adult mice against ZIKV and greatly reduces viral titers
- The vaccine protects fetuses against ZIKV challenge and reduces placental damage
- Depletion of CD8+ T cells abrogates vaccine protection in animal models

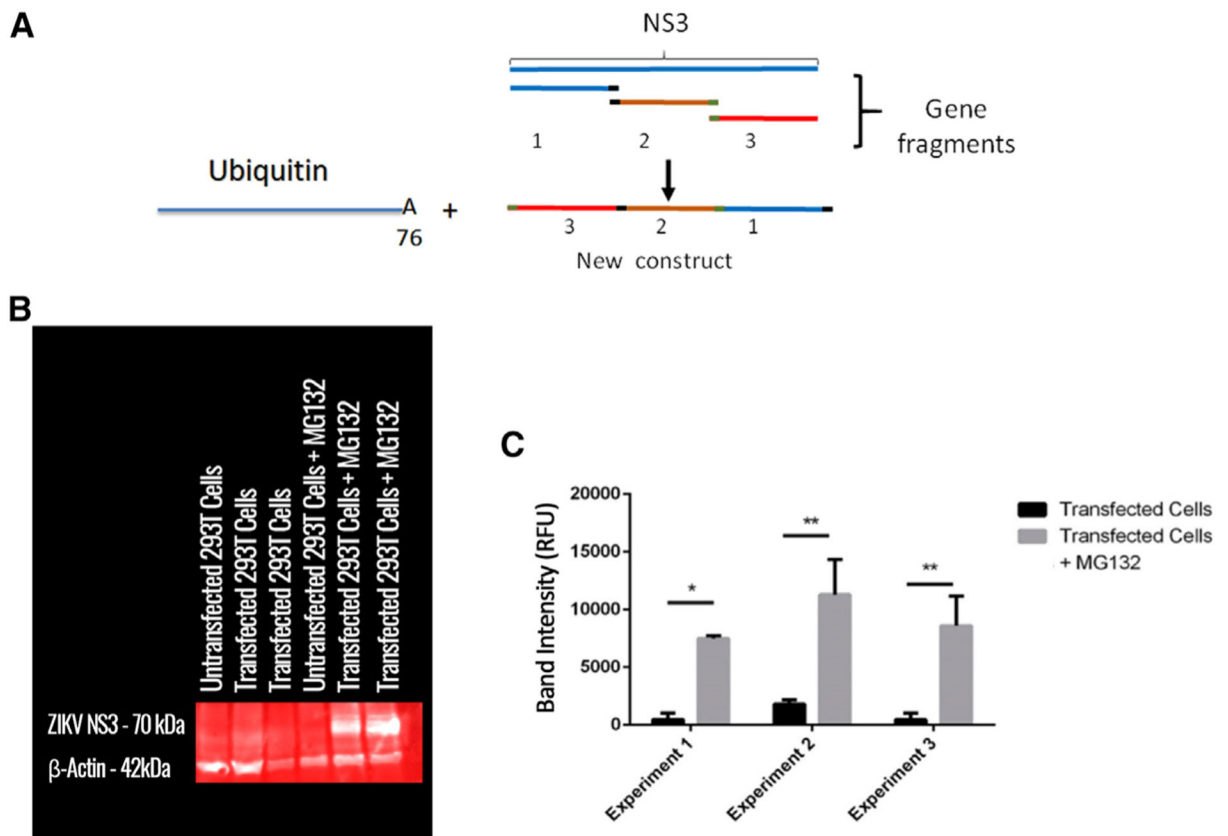


**Figure 1. ZIKV TCI vaccine design and antigen expression**

(A) Schematic diagram of plasmid design. The gene sequence encoding for the NS3 protein was split into three parts (denoted 1, 2, and 3). The 30 nucleotide bases before and after any cleaved sequence were placed in front of each region to preserve any epitopes that may have been disrupted. The ORF gene encoding for a mouse/human monomer of ubiquitin (Ub) was placed immediately upstream of the rearranged NS3 sequence. A glycine at the 76th residue was modified to encode an alanine to enhance the stability of the Ub/NS3 complex.

(B) 293T cells were transfected with the rearranged Ub/NS3 plasmid overnight. The cells were allowed to stably express plasmid for 36 h. After this period, MG132 was added overnight. The cell lysate was analyzed via western blot for the expression of NS3 and beta-actin. A representative blot from three experiments is shown.

(C) Total band density of western blot was quantified using ImageJ and analyzed using GraphPad (Prism). The data are represented as mean  $\pm$  SEM ( $n = 2$  for each experiment, three experiments total). \* $p < 0.05$ ; \*\* $p < 0.01$ .

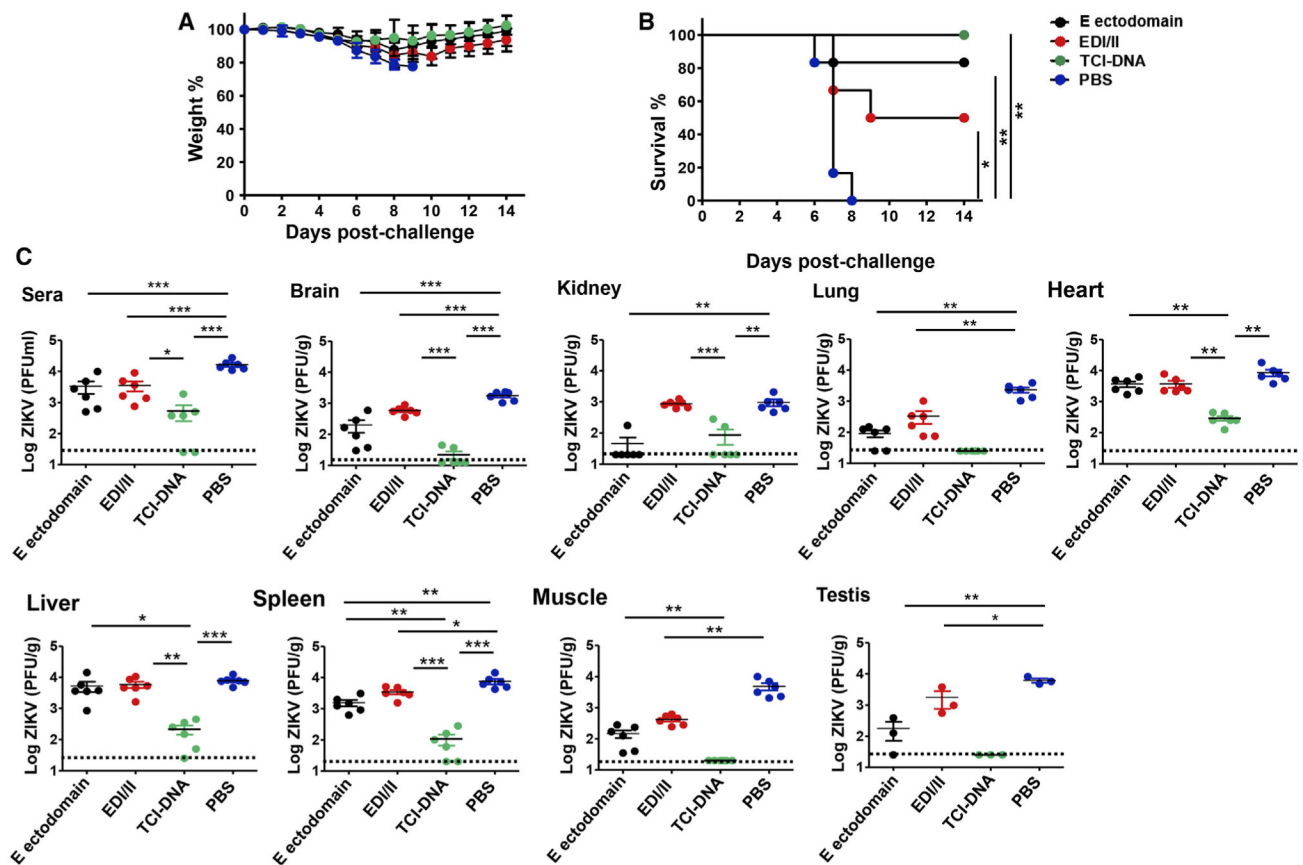


**Figure 2. ZIKV TCI-DNA vaccine protected adult male and female *Ifnar1*<sup>-/-</sup> mice against ZIKV challenge with complete survival and reduced viral titers, including reproductive organs**

Equal numbers of male and female *Ifnar1*<sup>-/-</sup> mice were immunized with ZIKV E ectodomain, EDI/II peptides, TCI-DNA, or PBS control, and sera were collected at 10 days post-second immunization.

(A and B) At 13 days post-second immunization, the mice were challenged (i.p.) with ZIKV (strain R103451, 10<sup>3</sup> PFU/mouse) and recorded for weight (A) and survival (B) daily for 14 days (n = 6).

(C) In a separate experiment, the immunized *Ifnar1*<sup>-/-</sup> mice were challenged with ZIKV (strain PAN2016, 10<sup>3</sup> PFU/mouse), and 6 days later, sera and tissues (including brain, kidney, lung, heart, liver, spleen, muscle, and testis) were collected for detection of viral titers using plaque-forming assay. The detection limit was 25 PFU/ml (for sera), 12.5 PFU/g (for brain), 20 PFU/g (for kidney, spleen, and muscle), and 25 PFU/g (for lung, heart, liver, and testis).

The data are represented as mean ± SEM (n = 3 for testis and n = 6 for other groups). \*p < 0.05; \*\*p < 0.01; \*\*\*p < 0.001.

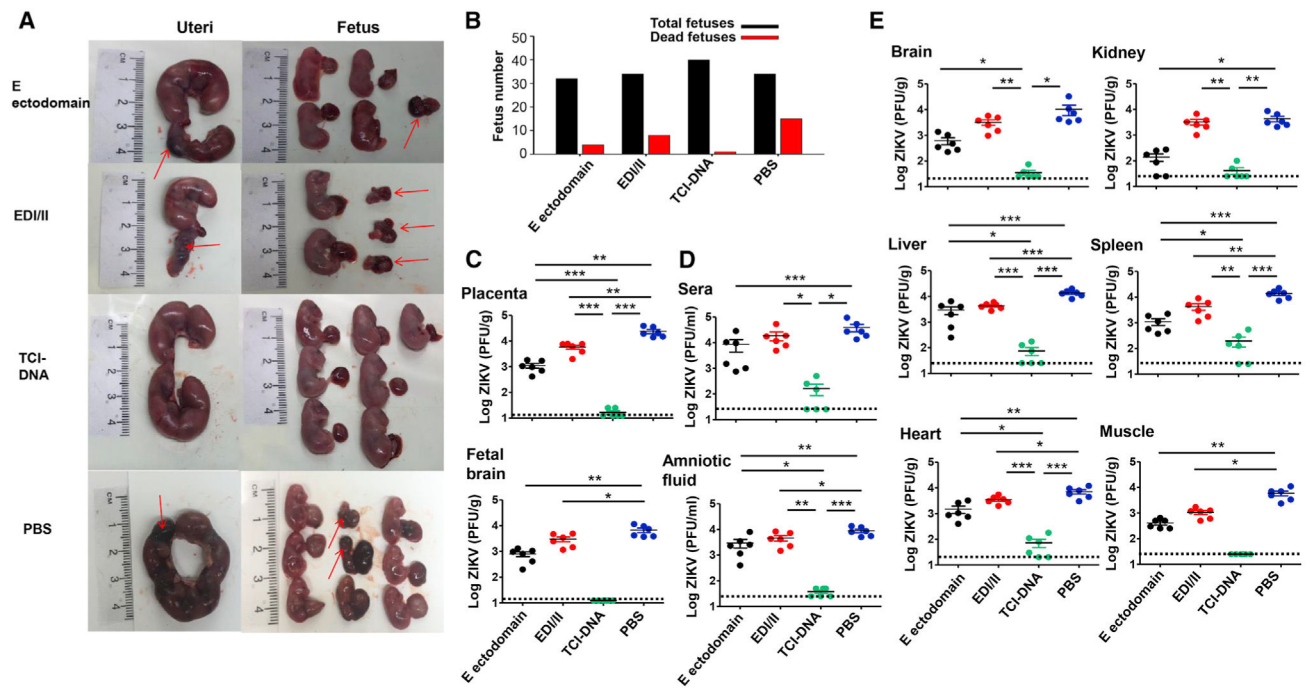


**Figure 3. ZIKV TCI-DNA vaccine protected female pregnant *Ifnar1*<sup>-/-</sup> mice and their fetuses against ZIKV challenge**

Female *Ifnar1*<sup>-/-</sup> mice were immunized with ZIKV E ectodomain, EDI/II peptides, TCI-DNA, or PBS control and mated with male *Ifnar1*<sup>-/-</sup> mice for pregnancy at day 10 post-second immunization. The pregnant mice (E10–E12) were challenged with ZIKV (strain R103451, 10<sup>4</sup> PFU/mouse), and 6 days later, uteri and fetuses were collected to evaluate morphological changes as well as sera, body fluid, and tissues (including placenta) to measure viral titers using plaque-forming assay. Placenta was also observed for apoptosis and vascular damage and examined for inflammatory cytokines and chemokines as described below.

(A and B) Representative image of morphology of uteri (E16–E18) and fetuses from pregnant mice challenged with ZIKV at E10–E12 (A), among which total numbers and dead fetuses from each group are shown (B).

(C–E) Viral titers in placenta, fetal brain (C), as well as sera and amniotic fluid (D) and tissues (including brain, kidney, liver, spleen, heart, and muscle) (E), 6 days post-challenge. The detection limit was 12.5 PFU/g (for placenta and fetal brain), 20 PFU/g (for heart), 25 PFU/ml (for sera and amniotic fluid), and 25 PFU/g (for brain, kidney, liver, spleen, and muscle).

The data are represented as mean ± SEM (n = 6). \*p < 0.05; \*\*p < 0.01; \*\*\*p < 0.001.

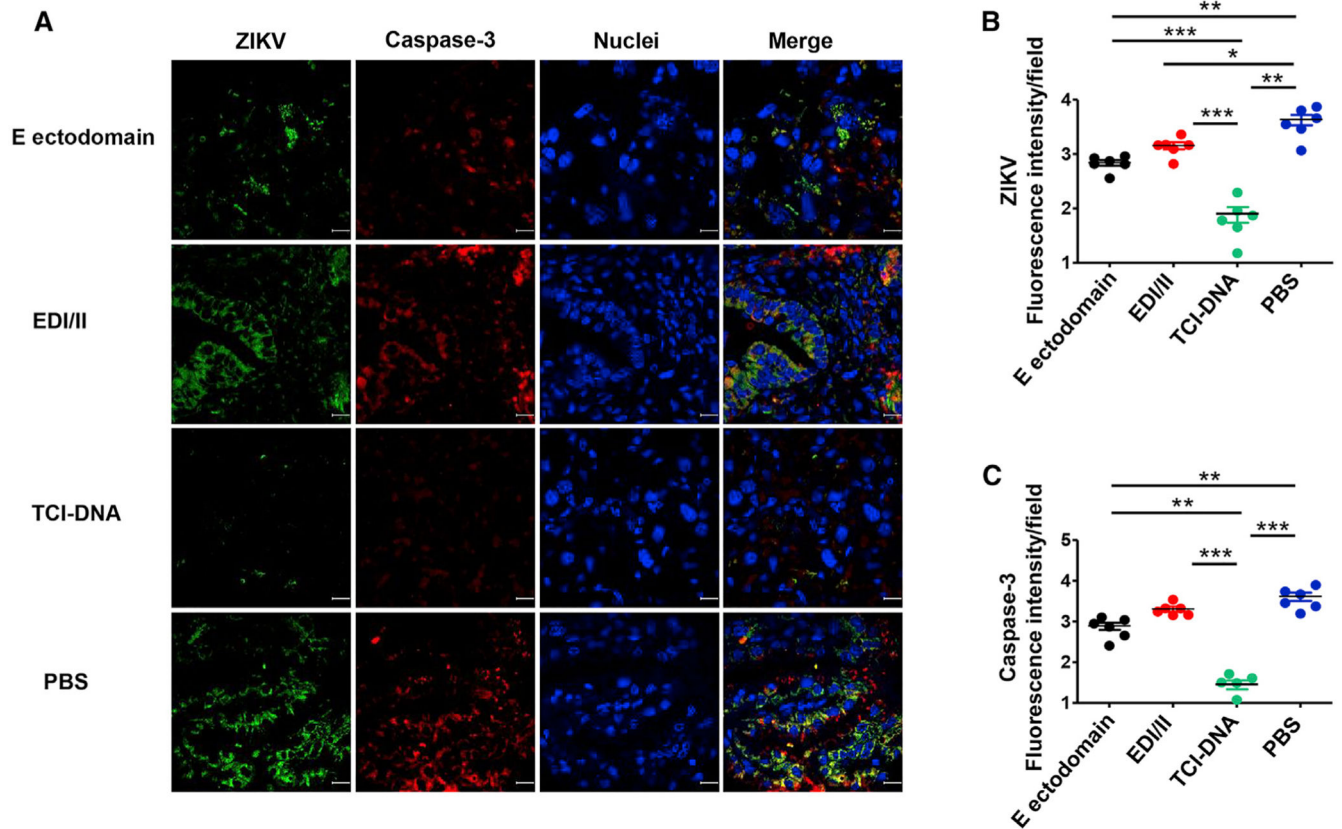


**Figure 4. ZIKV TCI-DNA vaccine prevented ZIKV-caused apoptosis in placenta of female pregnant *Ifnar1*<sup>-/-</sup> mice**

Placenta collected from above ZIKV-challenged pregnant (E10–E12) *Ifnar1*<sup>-/-</sup> mice was stained for activated form of caspase-3 (an apoptotic marker) by immunofluorescence assay.

(A) Representative images of immunofluorescence staining of activated caspase-3 in placenta. ZIKV (green), activated caspase-3 (red), and nuclei (blue) were stained with anti-ZIKV antibody, anti-active caspase-3 antibody, and DAPI, respectively. The images were magnified at 63 $\times$ , with a scale bar of 10  $\mu$ m.

(B and C) Quantification of ZIKV<sup>+</sup> (B) and activated caspase-3<sup>+</sup> (C) staining in (A) by ImageJ software.

The data are presented as mean  $\pm$  SEM of fluorescence intensity for ZIKV<sup>+</sup> or caspase-3<sup>+</sup> staining in each field (n = 6; n indicates numbers of images from different placentas). \*p < 0.05; \*\*p < 0.01; \*\*\*p < 0.001.

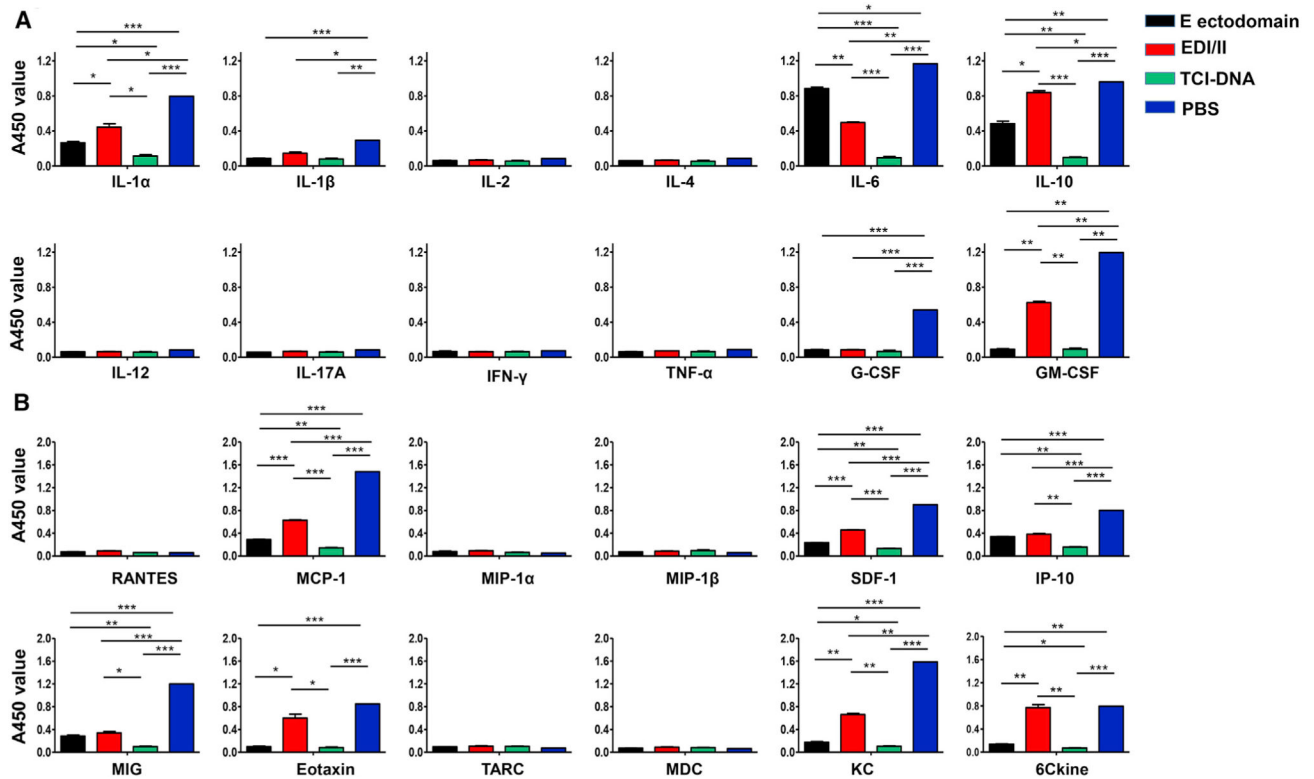


**Figure 5. ZIKV TCI-DNA vaccine prevented ZIKV-caused inflammation in placenta of female pregnant *Ifnar1*<sup>-/-</sup> mice**

Placentas collected from above challenged pregnant (E10–E12) *Ifnar1*<sup>-/-</sup> mice were examined for inflammatory cytokines (A) and chemokines (B) by Mouse Inflammatory Cytokines Multi-Analyte ELISArray Kit and Mouse Common Chemokines Multi-Analyte ELISArray Kit, respectively. The data are presented as mean  $\pm$  SEM (n = 6). \*p < 0.05; \*\*p < 0.01; \*\*\*p < 0.001.

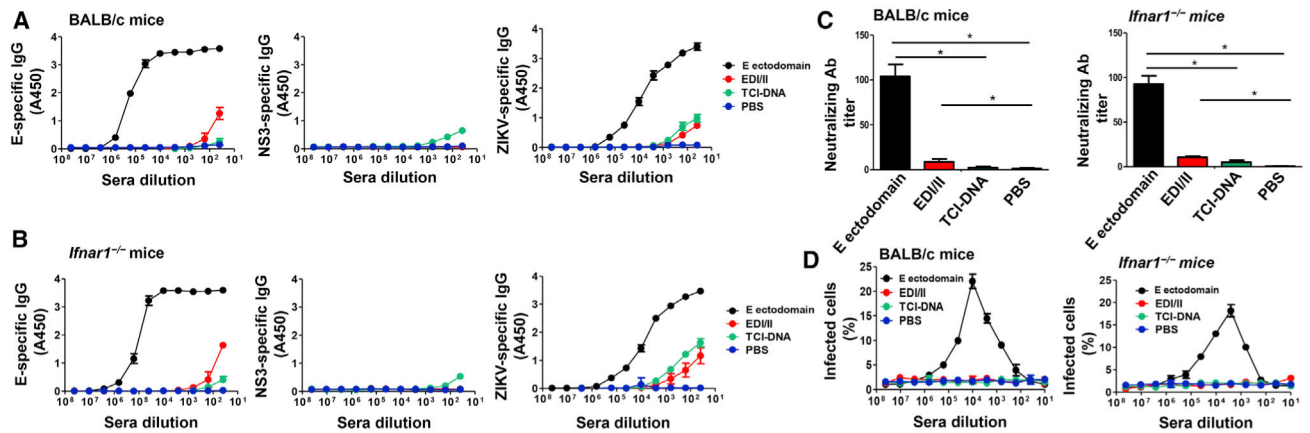


**Figure 6. ZIKV TCI-DNA vaccine induced low to no ZIKV-, E-, and NS3-specific antibodies without ADE effect**

Mouse sera collected at 10 days post-second immunization were detected for ZIKV E-, NS3-, and ZIKV-specific IgG antibody, neutralizing antibodies, and ADE of ZIKV infection. ZIKV strain R103451 was used for the neutralization and ADE tests.

(A and B) ELISA was used for detection of IgG antibody specific to ZIKV E ectodomain, NS3 peptides, and ZIKV (R103451 strain) in sera of BALB/c (A) or *Ifnar1*<sup>-/-</sup> (B) mice immunized with ZIKV E ectodomain, EDI/II peptides, TCI-DNA, or PBS control. IgG antibody titers are presented as positively detectable endpoint serum dilutions.

(C and D) Detection of neutralizing antibodies (C) by plaque-reduction neutralization test (PRNT) and ADE (D) by flow cytometry-based assay in sera of immunized BALB/c (left) or *Ifnar1*<sup>-/-</sup> (right) mice. Neutralizing antibody titers are presented as 50% PRNT titer (PRNT<sub>50</sub>) of 2-fold serially diluted sera. The ADE is presented as percent of infected cells, which was calculated based on fluorescence signals in the presence or absence of serially diluted sera.

The data are expressed as mean  $\pm$  SEM (n = 6). \*p < 0.01.

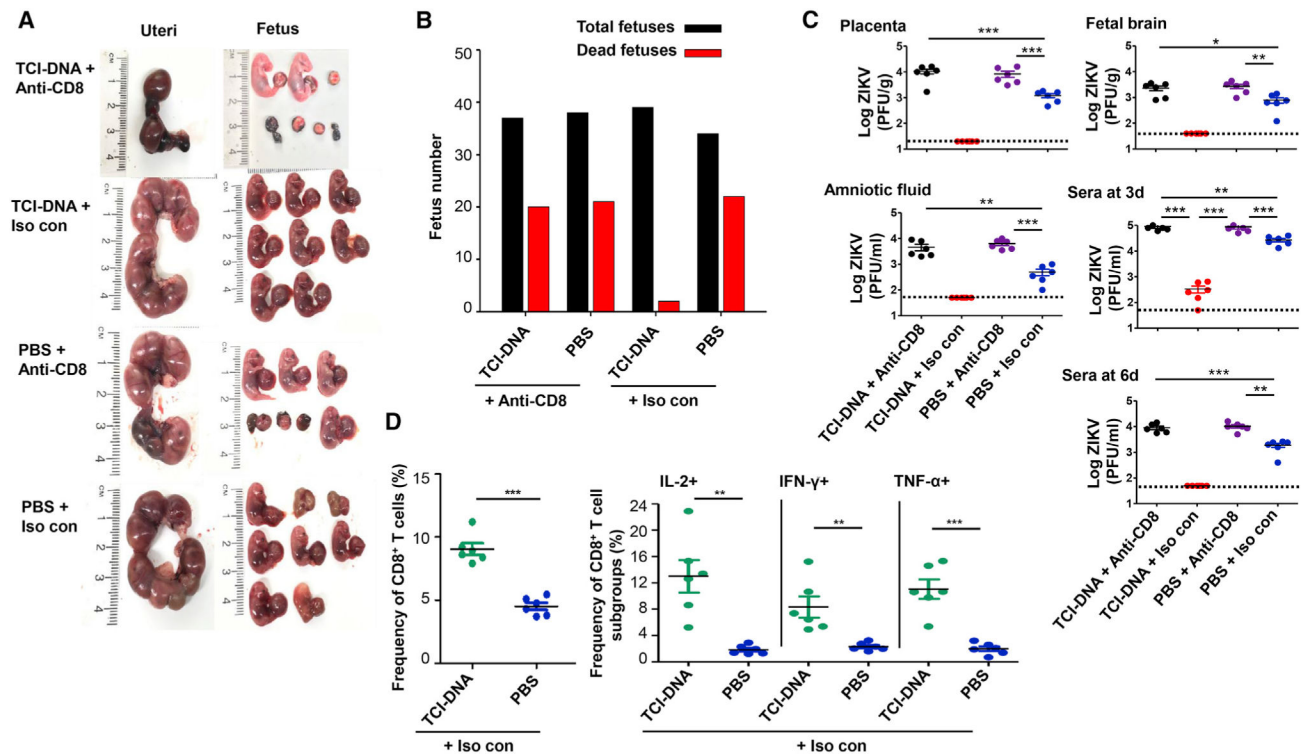


**Figure 7. CD8<sup>+</sup> T cell immune responses induced by ZIKV TCI-DNA vaccine played a key role in protecting pregnant mothers and their fetuses against ZIKV infection**

Female BALB/c mice were immunized with ZIKV TCI-DNA or PBS control for two doses and mated with male BALB/c mice for pregnancy at 10 days post-second immunization. The pregnant (E10–E12) mice were then injected (i.p.) with anti-CD8a (for depleting CD8<sup>+</sup> T cells) or IgG2a isotype control (i.e., Iso con; without depleting CD8<sup>+</sup> T cells) antibody (200  $\mu$ g/mouse) for three times (–2, –1, and 3 days p.i.). One day before challenge, the mice were also injected with anti-IFNAR1 blocking antibody (for depleting type I IFN; 2 mg/mouse) and then infected with ZIKV (strain R103451, 10<sup>6</sup> PFU/mouse).

(A–C) Six days post-challenge, the mice were euthanized, recorded for morphology of uteri and fetuses (A), and counted for dead and total fetuses (B), and viral titers were determined by plaque-forming assay in placenta, amniotic fluid, and fetal brain, as well as sera collected at 3 and 6 days post-challenge (C). The detection limit was 20 PFU/g (for placenta), 40 PFU/g (for fetal brain), and 50 PFU/ml (for sera and amniotic fluid). Six days post-challenge, splenocytes were isolated from the mice injected with isotype control antibody (i.e., Iso con) and analyzed for ZIKV-specific CD8<sup>+</sup> T cell responses by flow cytometry analysis.

(D) Quantification of the frequencies of CD8<sup>+</sup> T cells (left), as well as IL2<sup>+</sup>, IFN- $\gamma$ <sup>+</sup>, and tumor necrosis factor (TNF)- $\alpha$  secretion in CD8<sup>+</sup> T cells (right) in splenocytes.

The data are represented as mean  $\pm$  SEM (n = 6). \*p < 0.05; \*\*p < 0.01; \*\*\*p < 0.001.

## KEY RESOURCES TABLE

REAGENT or RESOURCE	SOURCE	IDENTIFIER
Antibodies		
Anti-mouse CD4 (IgG2b) antibody	Bio X Cell	BP0003-1; RRID:AB_1107636
Anti-mouse CD8a (IgG2b) antibody	Bio X Cell	BP0061; RRID:AB_1125541
Rat IgG2b isotype control antibody	Bio X Cell	BP0090; RRID:AB_1107780
Anti-mouse-CD8a (IgG2a) antibody	Bio X Cell	BE0004-1; RRID:AB_1107671
Rat IgG2a isotype control antibody	Bio X Cell	BE0089; RRID:AB_1107769
Anti-mouse IFNAR1 (MAR1-5A3) antibody	Leinco	I-401; RRID:AB_2491621
ZIKV EDIII-specific human antibody, ZV-64	Absolute Antibody	Ab00811-10.0
Rabbit anti-vimentin antibody	Abcam	Ab92547; RRID:AB_10562134
Rabbit anti-active caspase-3 antibody	Abcam	Ab2302; RRID:AB_302962
FITC-anti-human antibody	Sigma	9512-1mL; RRID:AB_259808
Anti-rabbit Alexa Fluor® 647 antibody	Abcam	Ab150075; RRID:AB_2752244
FITC-anti-mouse antibody	Biologend	406001; RRID:AB_315029
Anti-flavivirus 4G2 antibody	BEI Resources	NR-50327
PerCP-Cy5.5-anti-mouse CD8 antibody	BD Biosciences	551162; RRID:AB_394081
FITC-anti-mouse IL-2 antibody	BD Biosciences	554427; RRID:AB_395385
FITC-anti-mouse CD4 antibody	BD Biosciences	553729; RRID:AB_395013
PE-anti-mouse IFN- $\gamma$ antibody	BD Biosciences	554412; RRID:AB_395376
Brilliant Violet 421-anti-mouse TNF- $\alpha$ antibody	Biologend	506328; RRID:AB_2562902
HRP-conjugated anti-mouse IgG-Fab antibody	Sigma	a9917-1mL; RRID:AB_258476
Anti-ZIKV NS3 antibody	Genetex	GTX133309; RRID:AB_2756864
Bacterial and virus strains		
Zika virus (human strain R103451 (2015/Honduras))	BEI Resources	NR-50355
Zika virus (human strain PAN2016 (2016/Panama))	BEI Resources	NR-50210
Chemicals, peptides, and recombinant proteins		
Zika virus full-length envelope (E) protein	Aviva Systems Biology	OPMA04848
Zika virus EDI/EDII peptides (see below peptide 1-5)	BEI Resources	NR-50553
Peptide 1: IGVSNRDFVEGMSGG	BEI Resources	N/A
Peptide 2: TWVDVVLEHGGCVTV	BEI Resources	N/A
Peptide 3: MAQDKPTVDIELVTT	BEI Resources	N/A
Peptide 4: VDRGWGNGCGLFGKG	BEI Resources	N/A
Peptide 5: VVLGSQEGAVHTALA	BEI Resources	N/A
Zika virus NS3 overlapping peptides (see below peptide 6-15)	GenScript	N/A
Peptide 6: AETDEDHAHWLEARM	GenScript	N/A
Peptide 7: HAHWLEARMLLDNIIY	GenScript	N/A
Peptide 8: ARMLLDNIYLQDGLI	GenScript	N/A
Peptide 9: NIYLQDGLIASLYRP	GenScript	N/A
Peptide 10: GLIASLYRPEADKVA	GenScript	N/A
Peptide 11: YRPEADKVAAIEGEF	GenScript	N/A
Peptide 12: KVAAIEGEFKLRTEQ	GenScript	N/A

REAGENT or RESOURCE	SOURCE	IDENTIFIER
Peptide 13: GEFKLRTEQRKTFVE	GenScript	N/A
Peptide 14: TEQRKTFVELMKRGD	GenScript	N/A
Peptide 15: FVELMKRGDLPV	GenScript	N/A
Alum (Aluminum hydroxide gel)	InvivoGen	vac-alu-250
MPL (Monophosphoryl Lipid A)	InvivoGen	vac-mpla
Imiquimod	InvivoGen	vac-imq
Tween-20	Sigma	P1379-1L
Non-fat milk	Bio-Rad	1706404
TMB (3,3',5,5'-tetramethylbenzidine)	Sigma	T0440-1L
DMEM cell culture medium	Thermo Fisher Scientific	12430062
Fetal bovine serum (FBS)	ATLANTA biologicals	S11550
Penicillin/Streptomycin	Thermo Fisher Scientific	15140163
Carboxymethyl cellulose	Sigma	M0512-250G
Crystal violet	Sigma	C0775-100G
DAPI (4',6-diamidino-2-phenylindole)	Thermo Fisher Scientific	62247
Red Blood Cell Lysis Buffer	Biolegend	420301
Brefeldin A	Biolegend	420601
Molecular Biology Grade Water	Fisher	BP2819100
FastDigest EcoRI	Thermo Fisher Scientific	FD0274
FastDigest NotI	Thermo Fisher Scientific	FD0593
Certified Molecular Biology Agarose	Bio-Rad	1613102
T4 DNA Ligase	New England Biolabs	M0202T
DH5 $\alpha$ <i>E. coli</i>	In House	N/A
SOC Medium	Sigma	S1797-100mL
Kanamycin Solution	Sigma	K0254
Polyethylenimine Solution	Millipore Sigma	P3143
(R)-MG132	Millipore Sigma	M8699-1MG
Trypsin-EDTA (0.25%), phenol red	Thermo Fisher Scientific	25200056
Bio-Rad Protein Assay Dye Reagent Concentrate	Bio-Rad	5000006
12% Mini-PROTEAN TGX Precast Protein Gels	Bio-Rad	4561043
SuperSignal West Pico PLUS Chemiluminescent Substrate	Thermo Fisher Scientific	34579
Critical commercial assays		
FIX and PERM Cell Permeabilization Kit	Thermo Fisher Scientific	GAS004
Mouse Inflammatory Cytokines Multi-Analyte ELISArray	QIAGEN	336161
Mouse Common Chemokines Multi-Analyte ELISArray	QIAGEN	336161
Qiaquick Gel Extraction Kit	QIAGEN	28704
Qiaprep Spin Miniprep Kit	QIAGEN	27104

<b>REAGENT or RESOURCE</b>	<b>SOURCE</b>	<b>IDENTIFIER</b>
RNeasy Mini Prep Kit	QIAGEN	74104
GoScript Reverse Transcription System	Promega	A5003
iTaq Universal SYBRGreen Supermix	Bio-Rad	1725121
Experimental models: cell lines		
K562	ATCC	CCL-243
Vero E6	ATCC	CRL-1586
Experimental models: organisms/strains		
BALB/c mice	The Jackson Laboratory	651
Interferon- $\alpha/\beta$ receptor-deficient (Ifnar1 <sup>-/-</sup> ) mice	The Jackson Laboratory	32045-JAX
Software and algorithms		
GraphPad Prism 5	Graphpad Software	N/A
SigmaPlot 13.0	SigmaPlot Software	N/A
ZEN 2	Zen Software	N/A
ImageJ	NIH, USA	N/A

Author Manuscript

Author Manuscript

Author Manuscript

Author Manuscript